




Photocatalytic Reforming of Biomass: What Role Will the Technology Play in Future Energy Systems

Nathan Skillen¹ · Helen Daly² · Lan Lan² · Meshal Aljohani² · Christopher W. J. Murnaghan¹ · Xiaolei Fan² · Christopher Hardacre² · Gary N. Sheldrake¹ · Peter K. J. Robertson¹ 

Received: 22 April 2022 / Accepted: 27 May 2022 / Published online: 18 June 2022
© The Author(s) 2022

Abstract

Photocatalytic reforming of biomass has emerged as an area of significant interest within the last decade. The number of papers published in the literature has been steadily increasing with keywords such as ‘hydrogen’ and ‘visible’ becoming prominent research topics. There are likely two primary drivers behind this, the first of which is that biomass represents a more sustainable photocatalytic feedstock for reforming to value-added products and energy. The second is the transition towards achieving net zero emission targets, which has increased focus on the development of technologies that could play a role in future energy systems. Therefore, this review provides a perspective on not only the current state of the research but also a future outlook on the potential roadmap for photocatalytic reforming of biomass. Producing energy via photocatalytic biomass reforming is very desirable due to the ambient operating conditions and potential to utilise renewable energy (e.g., solar) with a wide variety of biomass resources. As both interest and development within this field continues to grow, however, there are challenges being identified that are paramount to further advancement. In reviewing both the literature and trajectory of the field, research priorities can be identified and utilised to facilitate fundamental research alongside whole systems evaluation. Moreover, this would underpin the enhancement of photocatalytic technology with a view towards improving the technology readiness level and promoting engagement between academia and industry.

Keywords Photocatalysis · Biomass · Hydrogen · Technology readiness level (TRL) · Energy

This article is part of the Topical Collection “Solar-driven catalysis”; edited by Nicolas Keller, Fernando Fresno, Agnieszka Ruppert and Patricia Garcia-Munoz. Provided Funding information has to be tagged.

Extended author information available on the last page of the article

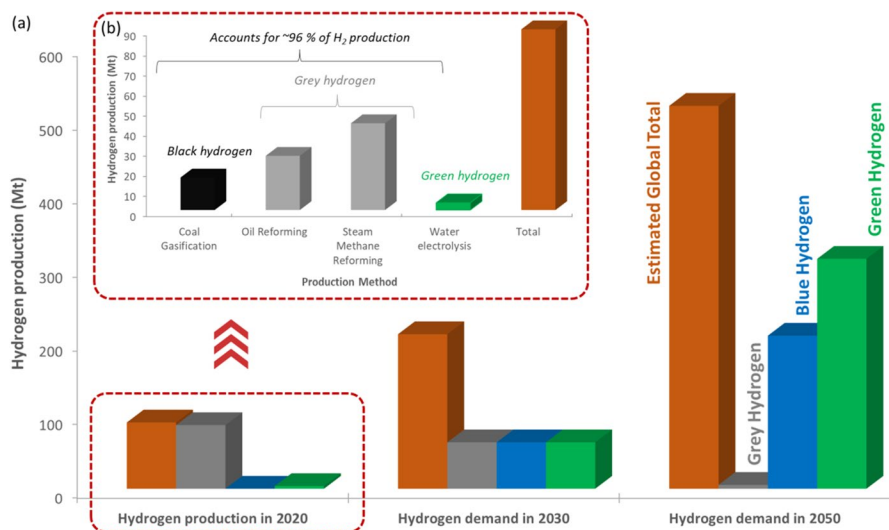


Fig. 1 (a) Current (2020) and future global H_2 production in relation to grey, blue and green H_2 generation along with (b) a breakdown of production methods for H_2 generation in 2020 including black, grey and green H_2 [2–5]

1 Introduction

1.1 A Future Low-Carbon Energy Landscape

Countries around the globe have now set ambitious net zero emission (NZE) targets with the aim of facilitating a transition towards a green, low-carbon society. In 2019, the UK became one of the first major economies to pass laws that aligned with these targets by requiring all greenhouse gas emissions to be net zero (in comparison to levels in 1990) by 2050 [1, 2]. Achieving these targets is beyond simply stating that it will be ‘challenging’. An approach must be deployed that encourages engagement across disciplines, technologies, sectors, industries, and governments—all of which must be underpinned by national and international strategies, continuous dissemination, and appropriate financial support. A key component within the transition to a low-carbon future is the role that hydrogen (H_2) will play in the global energy matrix. H_2 is also a unique example that highlights the challenge associated with the transition to a greener society. H_2 is already generated on a large global scale for use in industries such as refining, chemical synthesis and increasingly as an energy vector. The majority of that H_2 (~96%) is currently generated via fossil fuels (e.g., steam methane reforming (SMR) or coal gasification); however, to achieve NZE targets, governments are shifting their efforts towards H_2 produced via water electrolysis. This has given rise to categorising H_2 based on feedstock and manufacturing routes and resulted in the development of the ‘hydrogen rainbow’. The term has now been adopted by several governments and industries to help illustrate their sustainable strategy for transitioning from grey H_2 (fossil fuel derived) to green H_2 (water electrolysis with renewable electricity). Figures 1 and 2 show the

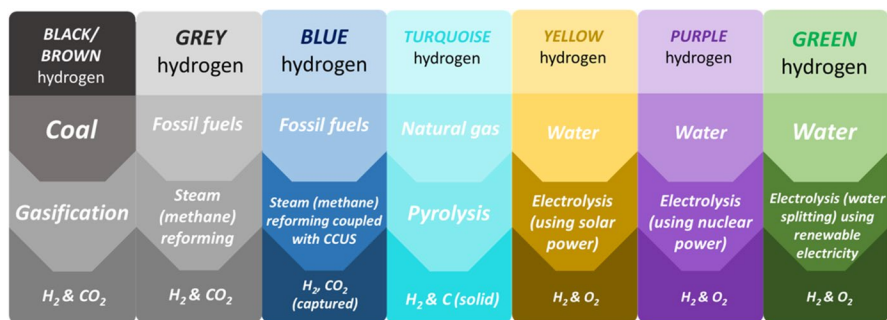


Fig. 2 An overview of the H₂ rainbow highlighting the feedstock, conversion process and output for each category

current manufacturing routes for global H₂ in 2020 along with the predicted increase in 2030 and 2050, and an overview of the H₂ rainbow, respectively.

To date, 17 countries have announced national H₂ strategies, which emphasises the level of intent directed towards establishing a strong H₂ economy. There is variation within each strategy; however, the majority have adopted a twin track approach wherein both green and blue H₂ are identified as primary methods for delivering low-carbon H₂ production (as indicated in the predicted demand for 2030 and 2050 in Fig. 1). In the UK specifically, a target capacity of 10 GW of low-carbon H₂ is set for 2030, with an intermediate target of 1 GW by 2025 [6]. A more immediate target is to complete feasibility testing to allow the use of up to 20% H₂ into the gas distribution grid for residential homes. According to the UK Government's hydrogen strategy, achieving these targets is predicted to create a UK H₂ economy that could be worth £900 million and generate 9000 high-quality jobs by 2030 [6]. In addition, modelling data suggest that 41 MtCO₂e could be saved between 2023 and 2032 as a result [5]. While ambitious, these strategies also highlight the uncertainty that still exists around H₂ deployment, specifically in relation to manufacturing routes, supply chains and the impact it could have on geopolitics. The International Energy Agency (IEA) predicted that to meet NZE by 2050, global H₂ production must achieve two substantial objectives [3, 4]:

- **An increase in production:** from 90 Mt in 2020 to > 200 and > 500 Mt in 2030 and 2050, respectively
- **A shift in manufacturing routes:** from 95% grey H₂ to 99% low-carbon production (e.g., a combination of blue and green H₂)

The uncertainty that has arisen is aligned with the fact that green H₂ production is still to be fully deployed at large scale as it currently accounts for only ~4% of global production. Furthermore, the cost of green H₂ remains high at ~7 p/kWh (compared to <4 p/kWh for SMR) and the current infrastructure in most countries would be unable to support a centralised distribution system [5]. It is, therefore, evident that alternative and complementary technologies will play a role in future energy

systems. As a result, innovation and technology development will be crucial in contributing towards achieving low-carbon H₂ production.

As a result of these challenges, increasing attention is being focussed on emerging technologies as alternative routes to H₂ production which can support an expanding H₂ economy at regional, national and international level. Along with research into thermolysis and redox chemistry [7], emerging technologies such as bioelectrolysis, biophotolysis and dark/photo-fermentation (as approaches to biohydrogen generation [8]) have gained significant attention in the literature. Beyond that, an area of particular interest is harnessing solar energy for the conversion of sustainable or waste feedstocks for H₂ generation. Technologies such as artificial photosynthesis and photocatalysis are seen as highly desirable approaches due to their ability to valorise a range of feedstocks to both energy and value-added products.

1.2 Photocatalytic Reforming of Biomass

Photocatalytic reforming of biomass has grown significantly to become one of the most rapidly evolving applications in the field. The earliest report of photocatalysis being deployed for biomass conversion was by Kawai and Sakata in 1980, who demonstrated that generation of H₂ from carbohydrates was occurring via photo-reforming [9]. In their work, the authors suggested that the carbon chains of compounds such as starch, sugar and cellulose were oxidised via reactions at the valence band (VB) which subsequently generated CO₂ and protons. The protons were then reduced by electrons at the conduction band (CB) to produce H₂. Despite this first paper being published alongside other early seminal work in photocatalysis [10–13], it is only within the last decade that a significant increase in publications has been observed. One of the primary drivers behind this has been the expansion of the bio-energy sector coupled with the focus on ensuring that sustainable and energy efficient processes are used for renewable energy generation. Furthermore, the ‘biorefinery concept’, which aims to achieve the production of both energy and value-added compounds from biomass, has highlighted that the sector could be reliant on using multiple conversion technologies [14–16]. Subsequently, this has led to an increase in the number of novel catalytic processes aimed at the valorisation of biomass. Interestingly, however, another key driver for photocatalysis has evolved from within the research field itself, especially in view of achieving sustainable H₂ production [17]. While global renewable energy targets and sector growth have undoubtedly facilitated increased focus on photocatalysis for bioenergy, as a substrate, total biomass represents a photocatalytic feedstock that is potentially more economically viable than traditional ones such as alcohols, sugars, and acids. Water splitting remains a ‘holy grail’ for photocatalytic H₂ production; however, with unfavourable thermodynamics (i.e., a large change in the Gibbs free energy with $\Delta G_0 = -238 \text{ kJ mol}^{-1}$) and the limitation of back reactions (H₂ and O₂ forming H₂O) [18], a more feasible approach is to deploy a sacrificial electron donor (SED) that can also supply protons. Previously, alcohols [19] and acids [20] have been used for this; however, biomass represents a potentially more sustainable and economically viable SED for photocatalytic systems. Moreover, the chemical and structural complexity of biomass can

provide the added benefit of generating value-added compounds (bioproducts) during the process.

The reactions which occur during photocatalysis have been extensively reviewed in a number of excellent papers in the literature [21–28] with the core mechanism often remaining the same, irrespective of application. Photocatalysis is a light driven chemical process which utilises oxidation and reduction reactions via the generation of an electron–hole pair. The photocatalytic mechanism with respect to biomass as the reaction substrate is shown in Fig. 3, which utilises TiO_2 as a model photocatalyst. Provided photon energy equal to or greater than the energy band gap (E_{bg}) of the absorbing material (i.e., the photocatalyst) is provided, ground state electrons can be promoted to higher energy levels and in doing so create an electron–hole pair (Fig. 3a). The migration of the electron–hole pair to the catalyst surface facilitates redox reactions with absorbed species. Using an aerated aqueous solution containing biomass as an example, the photogenerated charge carriers are capable of reacting with H_2O and dissolved O_2 on or near the surface to generate reactive species, e.g. a hydroxyl radical ($\bullet\text{OH}$), a superoxide anion ($\text{O}_2^{\bullet-}$) and H_2O_2 (Fig. 3b, c), providing the redox potential of the reactions are met (Fig. 3d).

In biomass photocatalysis, the role of reactive oxygen species (ROS) and the surface interaction become crucial considerations. Biomass substrates can, in theory, undergo oxidation via direct (Fig. 3b, i—reaction with the h_{VB}^+) and indirect (Fig. 3b, ii—reaction with the $\bullet\text{OH}$) mechanisms to form reaction intermediates. In principle, the $\text{O}_2^{\bullet-}$ generated from the electron scavenging at the CB can also react with biomass to form reaction intermediates (Fig. 3c, iv). While it is yet to be reported in the literature, the H_2O_2 pathway (Fig. 3c, v) may also contribute towards generating intermediates via $\bullet\text{OH}$ attack. These intermediates can vary significantly depending on the composition of the starting substrate and are also subject to complex reaction pathways, which are yet to be fully elucidated in the literature. If cellulose is considered as a standard biomass model compound, reaction intermediates (denoted in Fig. 3 as *oxidised products) can include sugars such as cellobiose, glucose, arabinose and erythrose, platform chemicals such as HMF, and organic acids such as acetic and formic acid [29–31]. Although the mechanism is not fully understood, it is generally accepted that biomass can act as an effective SED for photocatalytic systems. The irreversible oxidation which occurs subsequently leads to a supply of both electrons and protons, with the latter facilitating the generation of H_2 at the CB (Fig. 3c, iii). To enhance H_2 production, a co-catalyst (e.g., Pt, Ni, Au or Pd [20, 32, 33]) is typically used as a reaction centre to trap electrons (e^-_{tr}) with operation under an inert atmosphere (e.g., N_2 purged) removing competition from O_2 for scavenging the electron.

The growth of this area is primarily reflected in the literature, with the number of papers on photocatalytic biomass conversion increasing rapidly over the past decade. Moreover, research trends also highlight the shift from early work which focused on simple carbohydrate models (i.e., sugars) [35, 36] to more recent work which utilises raw biomass (i.e., lignocellulosic material) for H_2 [32, 37], with examples also demonstrating activity under solar irradiation [29, 38]. While these reports represent the advancement of the technology, they also highlight key challenges which must be addressed. The development and deployment of photocatalysis as a technique

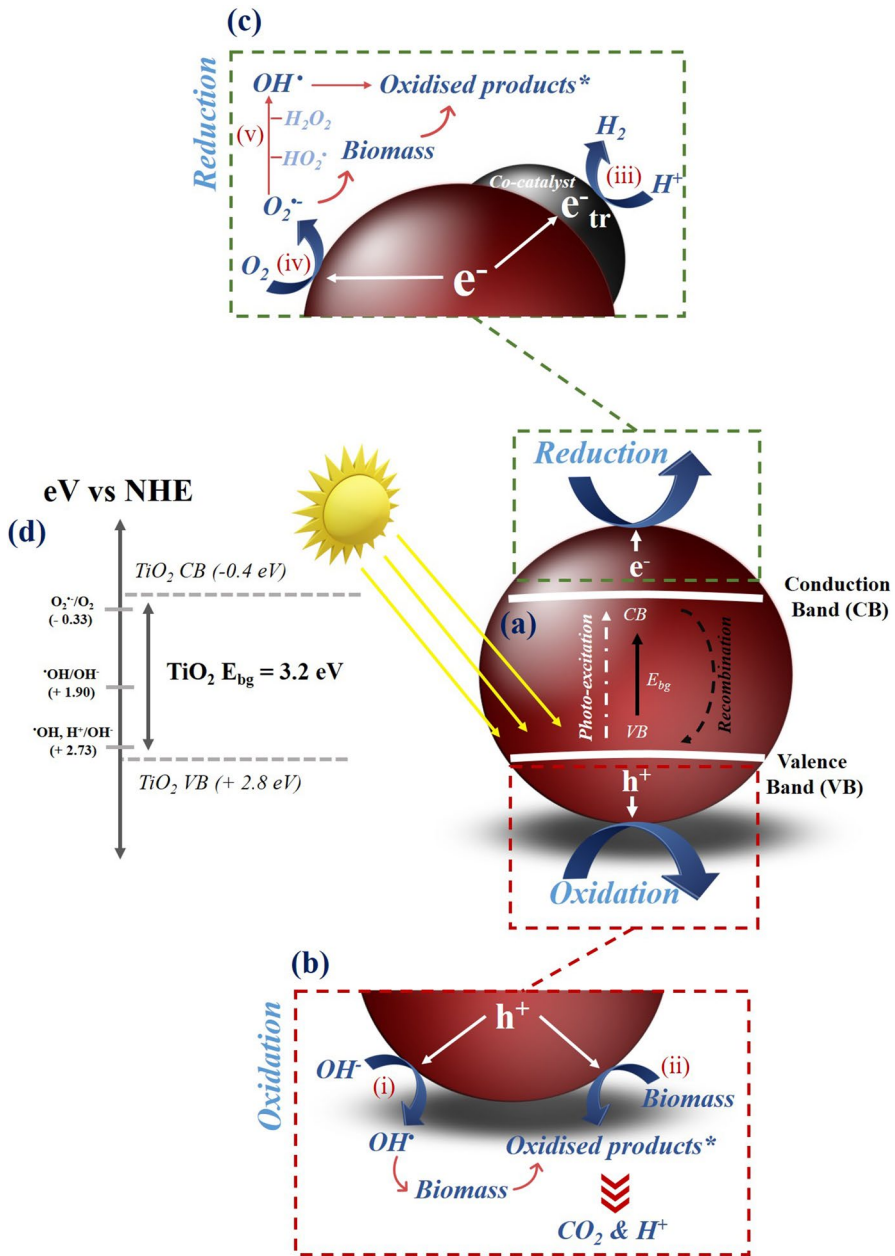


Fig. 3 An overview of the photocatalytic mechanism for biomass reforming including (a) the electronic structure of TiO_2 (as a model photocatalyst) and the processes of photo-excitation and recombination, the reactions which take place at (b) the valence band (including (i) radical attack and (ii) direct oxidation) (c) the conduction band (including (iii) H_2 generation, (iv) superoxide generation and (v) H_2O_2 formation) and (d) the redox potentials associated with the generation of reactive oxygen species. Please note * refers to a range of oxidised products which vary depending on the chemical structure of the biomass substrate. Adapted from [34] with kind permission from Elsevier

for biomass reforming is underpinned by not just overcoming these challenges, but by identifying a roadmap that will enhance the technology readiness with a view towards contributing to achieving net zero targets.

This article will explore these points in detail and provide a perspective on both the current state of the research and predicted future impact. A critical review is provided that evaluates current progress in the field which will be structured on product formation—specifically H_2 and value-added compounds. Following this, the article will focus on providing the reader with an outlook on future developments based on the previous critical evaluation. This includes identifying and categorising challenges and assessing the technology readiness level (TRL) of photocatalytic reforming of biomass before proposing a roadmap which outlines a strategy to facilitate future advancement of the technology. Biomass conversion is an emerging topic in photocatalytic research; however, to date, previous articles are either research-based or reviews of published research. For the first time in this field, this article evaluates the literature but also addresses the technology horizon and feasibility of the process for real-world deployment.

2 Current State of the Research

2.1 Photocatalytic H_2 Generation

Research on photocatalytic H_2 generation from biomass feedstocks, including cellulosic materials (i.e., cellulose, hemicellulose and lignin) and waste streams (e.g., wood, grass, and waste papers) are critically reviewed in this section. To accompany this, a comprehensive overview of the state-of-the-art information of photo-reforming of lignocellulosic materials is shown in Table 1. Unless otherwise stated, the generation of H_2 from such photocatalytic systems is assumed to proceed via the mechanism detailed in the previous section and in Fig. 3. The H_2 production (μmol) collected from the current literature was normalised by the amount of catalyst used (g_{cat}) and irradiation time (h) to obtain a H_2 production rate (r_{H_2} , $\mu\text{mol h}^{-1}g_{\text{cat}}^{-1}$), which was used for comparing the activity of photo-reforming of lignocellulosic materials over different catalysts or in different systems. Where appropriate, efficiencies (%) are also reported as either apparent quantum yields (AQY) or solar-to-hydrogen (STH). TiO_2 -based and non- TiO_2 -based (e.g., CdS-, ZnS-, CN_x -, carbon-based) catalysts were compared for their synthesis methods (as illustrated in Fig. 4) and activity of H_2 production (r_{H_2}) from photo-reforming of lignocellulosic materials. Photocatalytic reaction systems under the irradiation of solar simulators and natural sunlight are also reviewed based on their choices of photocatalysts, r_{H_2} and system design.

2.1.1 Photocatalysts for H_2 Production

TiO_2 is frequently used as a photocatalyst due to its suitable band gap energy (around 3.2 eV) under UV irradiation, and due to favourable characteristics such as its cost effectiveness, chemical stability and relatively low toxicity. While TiO_2

Table 1 The state-of-the-art data for the photocatalytic reforming of lignocellulosic materials

Photocatalyst	Substrate	Reaction conditions				T (°C)	Concentration (g L ⁻¹) ^b Catalyst	Substance/other solvent	H ₂ production rate ($\mu\text{mol h}^{-1}\text{g}_{\text{cat}}^{-1}$) ^c (%)(nm)	AQY/wavelength ^d	Other products	Refs
		Light source	P/I (W)/(mW cm ⁻²) ^a									
Pt/RuO ₂ /TiO ₂	Cellulose	Xe	500/–	25	7.5	3.0	–	12	0.3/380	CO ₂ , CH ₃ OH, C ₂ H ₅ OH	[9]	
Pt/TiO ₂	Cellulose	Xe	500/–	–	10	3.3	–	13	–	–	[63]	
Pt/TiO ₂	Cellulose	Xe	150/–	60	0.8	1.0	–	232	–	–	[32]	
Pt/TiO ₂	Cellulose	UV	4 × 15 W/–	–	2.0	6.7	–	225	–	Glucose, HMF	[46]	
Pt/TiO ₂	Cellulose	Simulator	–/25	–	2.0	6.7	–	185	–	–	[46]	
Pt/TiO ₂	Cellulose	Sunlight	–/45 (2.5) ^e	–	2.0	6.7	–	196	–	–	[46]	
Pt/TiO ₂	Cellulose	UV	250/–	130	2.0	0.1/0.6 M sulfu- ric acid	–	752	–	HMF	[45]	
mPt/TiO ₂	Cellulose	Xe	300/–	40	1.5	1.0% w/v ^f	–	600	9.6/365	–	[40]	
Pt/TiO ₂	Cellulose	Xe	300/–	40	1.5	1.0% w/v /HCl	–	900	14.5/365	–	[41]	
Pt/TiO ₂	Cellulose I	UV LED	13.2/5	28.5	0.75	4	–	40	3.9/–	–	[42]	
Pt/TiO ₂	Cellulose II	UV LED	13.2/5	28.5	0.75	4	–	104	9.4/–	–	[42]	
Pt/TiO ₂	Cellulose I	UV	16/	40	0.75	1	–	107	25.9/365	CO ₂	[64]	
Pt/TiO ₂	Cellulose II	UV	16/	40	0.75	1	–	177	42.8/365	CO ₂	[64]	
Pt/TiO ₂	Cellulose	UV	16/–	40	0.75	1	–	133	–	CO ₂	[43]	
Pt/TiO ₂	Cellulose	Xe	300/–	–	0.4	4	–	275	1.9/380	Lactic acid, arabinose, glu- cose, mannose, galacturonic acid	[47]	
Pt/TiO ₂	Cellulose	UV–Visible lamp	150/–	–	1	3.3	–	1456	–	–	[44]	

Table 1 (continued)

Photocatalyst	Substrate	Reaction conditions				H ₂ production rate	AQY/wavelength ^d	Other products	Refs
Ni-S/TiO ₂	Cellulose	Xe	500/400	80	0.2	10.0	–	Arabinose, galactose, glucose, xylose, formic acid	[48]
Au/HYT ^g	Cellulose	Visible	–/0.5	140	0.1	0.1/EMIMCl ^h	–	Glucose, HMF	[65]
TiO ₂ film	Cellulose	UV	–/–	–	9 coatings	100/ZnCl ₂	–	HMF	[66]
Cellulose@Pt/TiO ₂	Cellulose	UV	250/–	40	0.3	–	–	Glucose, formic acid	[29]
NiP ₂ -NCN _x ⁱ	Cellulose	Simulator	–/100	25	5.0 mg	10.0 M/KPi ^j	–	–	[52]
NiS/CdS	Cellulose	Xe lamp	300/–	–	1	10	–	–	[50]
CdS/CdO _x QDs ^k	Cellulose	Simulator	–/100	25	0.5 μM	50/10 M, KOH	1.2/430	–	[38]
Pt/SGODs ^l	Cellulose	Simulator	–/100	–	0.8	4/10 M, NaOH	23.3/420	HCOO [–] , C6 to C1	[57]
CdS/CdO _x QDs	Hemicellulose ^m	Simulator	–/100	25	0.5 μM	0.25/10 M, KOH	1.2/430	–	[38]
NiP ₂ -NCN _x	Hemicellulose ⁿ	Simulator	–/100	25	1.6	33.3/4.3 M, KPi	–	–	[52]
Pt/g-C ₃ N ₄	Hemicellulose	Xe	300/100	5	5	5/pH = 10	–	–	[53]
Pt/TiO ₂	Lignin	Xe	500/–	–	10	3.3	–	–	[67]
TiO ₂ @NiO	Lignin ^o	Xe	300/	60	0.5	4/1 M, NaOH	–	CH ₄ , fatty, palmitic, stearic and butanedioic acids	[49]

Table 1 (continued)

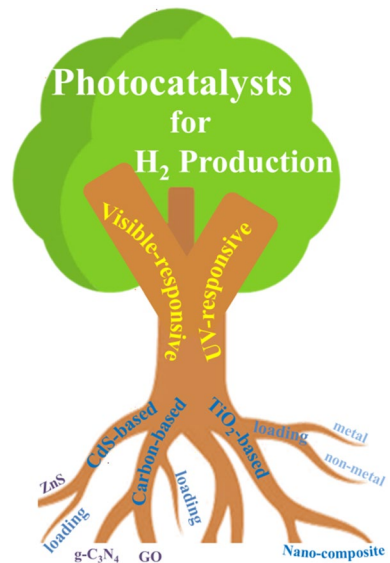
Photocatalyst	Substrate	Reaction conditions	H ₂ production rate	AQY/wavelength ^d	Other products	Refs
C,N,S-doped ZnO/ZnS	Lignin ^p	Xe 300/-	0.1 0.5	15.1/-	1-phenyl-3-buten-1-ol	[68]
CdS/CdO _x QDs	Lignin	Simulator -/100	0.25/10 M, KOH 0.5 μM	1.2/430	-	[38]
NiP ₂ -NCN _x	Lignin	Simulator -/100	1.6 40.8	-	-	[52]
Pt ₂ -NCN _x	Lignin	Simulator -/100	1.6 14.5	-	-	[52]
Pt/g-C ₃ N ₄	Lignin	300/100 Xe	5 20.75	-	-	[53]
NiS/CdS	Lignin	300/ Xe	1 147.6	44.9/-λ, ≥400 nm	-	[51]
Pt/TiO ₂	Poplar wood	300/- Xe	0.4 26	-	-	[47]
Pt/TiO ₂	Pinewood	Simulator -/200	30.0 -/HCl	1.1 ^p	-	[58]
Pt/TiO ₂	Fescue grass	300/- Xe	0.8 68	-	-	[32]
Pt/TiO ₂	Rice husk	UV -/	2 100	-	-	[46]
Pt/TiO ₂	Alfalfa stem	UV -/	2 100	-	-	[46]
Pt/TiO ₂	Paper pulp	UV 250/-	130 0.5	1320	-	[45]
CdS/CdO _x QDs	Grass	Simulator -/100	0.5 M 900	-	-	[38]
CdS/CdO _x QDs	Printer paper	Simulator -/100	0.5 M 1050	-	-	[38]
CdS/CdO _x QDs	Cardboard	Simulator -/100	0.5 M 680	-	-	[38]
CdS/CdO _x QDs	Newspaper	Simulator -/100	0.5 M 320	-	-	[38]
CdS/CdO _x QDs	Wooden branch	Simulator -/100	0.5 M 5350	-	-	[38]
CdS/CdO _x QDs	Bagasse	Simulator -/100	0.5 M 250	-	-	[38]
CdS/CdO _x QDs	Sawdust	Simulator -/100	0.5 M 720	-	-	[38]

Photocatalyst	Substrate	Reaction conditions	H ₂ production rate	AQY/wavelength ^d	Other products	Refs	
NIP-, ^{NCN} CN _x	Sawdust	Simulator	25	1.6	0.16/4.3 M, KPi	202	[52]
NIP-, ^{NCN} CN _x	Paper	Simulator	25	1.6	0.16/4.3 M, KPi	42.7	[52]
NIP-, ^{NCN} CN _x	Cardboard	Simulator	25	1.6	0.16/4.3 M, KPi	46.9	[52]
NIP-, ^{NCN} CN _x	Bagasse	Simulator	25	1.6	0.16/4.3 M, KPi	34.8	[52]
NIP-, ^{NCN} CN _x	Wooden branch	Simulator	25	1.6	0.16/4.3 M, KPi	35.7	[52]

^aLight intensity was shown in two units in the literature, i.e., in radiant flux power (P), or in irradiance (I)
^bDefault unit is g L⁻¹ if there is no noted unit following the value. Various units were noted as they were shown in different ways in the original literature
^cSolvents (other than water) were used to dissolve the substrates or adjust the pH of the system
^dThe production rate of H₂ is the amount of H₂ produced per hour (μmol h⁻¹) normalised by the amount of catalyst (g) used in the studies
^eAQY is the abbreviation for apparent quantum yield, which is calculated by the ratio of the molar mass of transferred electrons to the molar mass of incident photons
^fThe average solar power of the natural sunlight used in this study was 45 mW cm⁻² in the visible range and 2.5 mW cm⁻² in the UV range

^gw/v represents the weight/volume percentage concentration
^hHYT is the abbreviation of TiO₂ nanofibres supported H-form Y-zeolites (HY) catalyst
ⁱEMIMCl is 1-ethyl-3-methylimidazolium chloride ionic liquid solution which is used to dissolve cellulose as a pre-treatment in this study
^jNIP-,^{NCN}CN_x is the bulk cyanamide-functionalised carbon nitride (^{NCN}CN_x) with molecular Ni bis(diphosphine) (NIP) as the co-catalyst
^kKPi is a potassium phosphate solution used in this study
^lQDs is the abbreviation of quantum dots, and (Co(BF₄))₂ is used as the co-catalyst in this study
^mSGODs is the abbreviation of the S- and N-doped grapheme oxide dots (SGODs)
ⁿThe hemicellulose used in this study is xylan from beech wood
^oThe hemicellulose used in this study is xylan
^pKraft lignin was used as the lignin source in this study
^qSodium salt lignisulfonate was used as the lignin source in this study
^rThe solar-to-H₂ efficiency is calculated by the ratio of calculated energy corresponding to H₂ volume generated by taking into account the energy content of H₂ (142 MJ/kg) to the energy supplied during photocatalysis at different irradiation intensities

Fig. 4 Illustration overview of common photocatalysts and their synthesis strategies for H_2 production from photocatalytic reforming of lignocellulosic materials



has previously been reported as non-toxic, it is worth noting that as of 2021, the European Union classified TiO_2 as a suspected carcinogen (category 2) by inhalation. The activity of bare TiO_2 for H_2 production from photocatalytic reforming of lignocellulosic materials, however, is relatively low, mainly as a result of the rapid recombination of photogenerated electrons (e_{CB}^-) and holes (h_{VB}^+) [39]. In the initial work by Kawai and Sakata, improvements on the efficiency of separating e_{CB}^- and h_{VB}^+ was achieved by physically mixing and grinding the powders of RuO_2 , TiO_2 and Pt together [9]. This mixed catalyst was then suspended, with cellulose, in H_2O for H_2 production under the irradiation of a Xe arc lamp. This first study showed the feasibility of cellulose as a SED in photo-reforming wherein H_2 production of $12 \mu mol h^{-1} g_{cat}^{-1}$ was achieved. The efficiency and yields of H_2 production with cellulose as an SED are compared in Table 1 with the enhanced performance mainly achieved through catalyst synthesis strategies such as (i) optimisation of metal or non-metal co-catalyst loading on the TiO_2 support, and (ii) fabricating novel TiO_2 -based composites.

Wet impregnation [32, 40–44] and photodeposition [45–47] methods are frequently used for loading metals (e.g., Pt, Au or Pd) as the co-catalyst onto a TiO_2 support, with Pt the most commonly studied. As shown in Table 1, the rH_2 of these noble metal loaded TiO_2 catalysts for photo-reforming of lignocellulosic materials are in the range of 100–1000 $\mu mol h^{-1} g_{cat}^{-1}$. While the activity can obviously be enhanced by loading noble metals, the high costs of such materials have implications on the commercial and economic viability at scale. Non-noble metal (or non-metal) species have also been introduced onto TiO_2 supports for H_2 generation via photo-reforming of cellulose. Hao et al. [48] successfully prepared a Ni-S/ TiO_2 catalyst on which sulfate (SO_4^{2-}) and nickel sulfide (Ni_xS_y) were chemisorbed onto the TiO_2 . The rH_2 (3020 $\mu mol h^{-1} g_{cat}^{-1}$) was significantly improved, by 96 times, after

loading both Ni_xS_y and SO_4^{2-} on TiO_2 . This enhancement could be due to the synergistic role of both Ni_xS_y and SO_4^{2-} ; the Ni_xS_y served as both electron trap and co-catalyst for H_2 evolution, while binding SO_4^{2-} generates acidic sites in the catalyst which can facilitate insoluble cellulose hydrolysis to soluble glucose, which is more efficient for quenching photogenerated holes and providing protons.

Novel TiO_2 -based composite structures have also been developed for H_2 generation via the photo-reforming of lignocellulosic materials. A TiO_2 @NiO core-shell composite was prepared by mixing $\text{Ti}(\text{OC}_3\text{H}_7)_4$ and $\text{Ni}(\text{CH}_3\text{COO})_2$ in acetic acid with hydrothermal (180 °C for 12 h) and calcination (600 °C for 2 h) treatments [49]. This nanocomposite was capable of generating H_2 ($r\text{H}_2 = 78 \mu\text{mol h}^{-1} \text{g}_{\text{cat}}^{-1}$) from lignin photo-reforming due to the synergistic effects between ultrafine nanoparticles, high crystallinity, core-shell structure with close contact and a n-p heterojunction which facilitated the efficient separation of the photogenerated electron-hole pair. Additionally, Zhang et al. prepared a cellulose-immobilised Pt/ TiO_2 (cellulose@Pt/ TiO_2) composite by filtering a mixed colloidal suspension of cellulose and platinised TiO_2 [29]. The study also compared a physically mixed cellulose and Pt/ TiO_2 (cellulose + Pt/ TiO_2) sample with the composite cellulose@Pt/ TiO_2 material (with both containing the same amounts of cellulose) for their activity of producing H_2 from cellulose photo-reforming. The $r\text{H}_2$ was approximately $933 \mu\text{mol h}^{-1} \text{g}_{\text{cat}}^{-1}$ over the cellulose@Pt/ TiO_2 while the value was negligible over the cellulose + Pt/ TiO_2 sample, which indicated the importance of interaction between cellulose and the Pt/ TiO_2 for efficient photocatalytic H_2 production. This could be due to the efficient transfer of photogenerated charge carriers (e_{CB}^- and h_{VB}^+) and ROS (i.e., $\bullet\text{OH}$) within the system.

Visible light-responsive photocatalysts such as sulfides ($E_{\text{bg}} = \sim 2.4$ eV CdS [38, 50, 51]) and carbon nanomaterials ($E_{\text{bg}} = \sim 2.7$ eV for graphitic carbon nitride [52, 53]) have also been developed for H_2 generation from photo-reforming of lignocellulosic substrates. 1D CdS nanowires (NWs) were prepared and loaded with NiS_2 by a two-step hydrothermal method. This catalyst showed visible light ($\lambda \geq 400$ nm) reactivity towards H_2 generation from photo-reforming of cellulose [50] and lignin [51] with a $r\text{H}_2 = 53$ and $147.6 \mu\text{mol h}^{-1} \text{g}_{\text{cat}}^{-1}$, respectively, where lactic acid was coexistent with lignin as a hole scavenger [47], whereas cellulose was used as the single hole scavenger [46] over NiS_2/CdS catalysts. The NiS_2 loading on CdS NWs was reported to enhance light absorption and charge transfer, which resulted in the visible light activity in producing H_2 . In addition to CdS NWs, CdS quantum dots were also reported to achieve high rates of H_2 evolution from photo-reforming of lignocellulosic materials ($r\text{H}_2 = 2300, 2000,$ and $260 \mu\text{mol h}^{-1} \text{g}_{\text{cat}}^{-1}$ for cellulose, hemicellulose, and lignin respectively) and even raw biomass ($r\text{H}_2 = 900$ and $720 \mu\text{mol h}^{-1} \text{g}_{\text{cat}}^{-1}$ for grass and sawdust respectively) in highly basic conditions (10 mol L^{-1} KOH) [38]. The high rates of H_2 production for this catalyst could be due to the coverage of CdO_x on CdS which promotes the binding between the substrates and photocatalyst. This resulted in effective H^+ transfer and weakening of C-C bonds, which in turn led to oxidation of the substrates and H_2 production. Consideration of the overall sustainability and environmental impact of the production of photocatalytic H_2 , however, would require inclusion of the catalyst synthesis/

precursors. Therefore, use of more environmentally benign metals in the preparation of active photocatalysts would be required.

Carbon nanomaterials are normally non-toxic with a suitable band gap (e.g., 2.7 eV for graphitic carbon nitride, g-C₃N₄ [54]) for absorbing visible light irradiation due to their 2D conjugated π -system. Activated carbon nitride (^{NCN}CN_x) was synthesised by an ultrasonication approach of breaking down aggregates of carbon nitride [52]. Cellulose, lignin, and raw biomass substrates were photo-reformed to H₂ over ^{NCN}CN_x (NiP as the co-catalyst) under the irradiation of a solar simulator, which demonstrates nontoxic, noble-metal free, and visible-light-promoted photo-reforming of lignocellulosic materials. Rao et al. [53] reported a monolayer g-C₃N₄ prepared by nitrogen-protected ball-milling of bulk g-C₃N₄ in water, which showed activity towards photo-reforming of lignin and hemicellulose to H₂ driven by visible light; the rH_2 was 60 (hemicellulose) and 20.8 (lignin) $\mu\text{mol h}^{-1} \text{g}_{\text{cat}}^{-1}$, with Pt as the co-catalyst. For 2D layered carbon-based materials, a thinner layered structure could result in larger surface area and more active sites, which would enhance activity for producing H₂ from photocatalytic reaction [54]. An increased band gap energy, however, could also be found with a thinner layer of this material due to quantum confinement effects by shifting the VB and CB in opposite directions [55]. Therefore, modification of g-C₃N₄ still needs to be developed to achieve enhanced performance in the production of H₂ from the photo-reforming of lignocellulosic materials under visible-light irradiation. In addition, in the development of photocatalysts for photo-reforming of lignocellulosic substrates, consideration must be given to the nature of the feedstock used when comparing the activities of photocatalysts. The rH_2 , particularly for lignin resources can vary significantly with reaction conditions (i.e., acid/alkaline/neutral solutions and concentration of substrate) as well as the solubility of the lignin resource (for example lignosulfonate, organosolv or kraft lignin compared to raw biomass). One of the highest rH_2 reported for lignin is for a C-, N-, and S-doped mixed phase ZnO and ZnS photocatalyst (C, N, S-ZnO/ZnS), prepared via calcination of bis-thiourea zinc acetate mixture, which demonstrated an rH_2 of 6430 $\mu\text{mol h}^{-1} \text{g}_{\text{cat}}^{-1}$ from photo-reforming of sodium lignosulfonate salt under visible-light irradiation [50]. In comparison, however, for raw biomass the rH_2 is typically below 1000 $\mu\text{mol h}^{-1} \text{g}_{\text{cat}}^{-1}$, for both UV and visible activation (Table 1).

2.1.2 Solar Irradiation

Sunlight is a sustainable source of energy; therefore, the efficient use or transfer of solar energy has been regarded as a promising and renewable approach to replace more traditional energy sources (e.g., fossil fuels) [56]. Photo-reforming of lignocellulosic materials for H₂ production under natural sunlight represents an ideal method to transfer the solar energy to low carbon H₂. Within the spectrum of natural sunlight, UV light represents only a small portion (~3–5% on an energy basis [39]) with the rest of the solar spectrum comprising wavelengths in the visible and infrared region. Therefore, in order to utilise natural sunlight efficiently, the development of visible light-responsive photocatalysts and the design of photoreactors which can fully harvest the irradiation of natural sunlight needs to be achieved.

Several studies reported in the literature have used solar simulators to mimic natural sunlight by adding an air mass filter (AM1.5G) to adjust the spectrum of a Xe arc lamp to the standard solar irradiation at ground level, with an approximate light intensity of 100 mW cm^{-2} [38, 52, 57, 58]. Such systems have been reported for the photo-reforming of biomass (i.e., cellulose, lignin, and raw biomass) over visible light responsive catalysts such as CdS/CdO_x quantum dots [38] and NiP^{NCN}CN_x [52]. H₂ was produced over both catalysts and with various substrates including cellulose, hemicellulose, lignin, and raw biomass (shown in Table 1). Additionally, the effect of the illumination wavelength of the solar simulator on the efficiency of producing H₂ was illustrated by an apparent quantum yield (AQY) in the photo-reforming of cellulose [57]. The results showed that both AQY and absorbance decreased with the irradiation wavelength, i.e., the AQY of 23.3% was achieved at 420 nm, and it decreased to 3.4% at 550 nm. The authors stated that this trend could be due to the low probability of the charge excitation under long-wavelength illumination.

Reports on using natural (and direct) sunlight as the irradiation source for producing H₂ from photo-reforming of biomass are limited [29, 46]. A system containing an aqueous cellulose suspension with a Pt/TiO₂ catalyst was irradiated under natural solar light (Pavia, 45°11'N, 9°09'E, July 2013, temperature 29–32 °C) for monitoring H₂ production [46]. A r_{H_2} of $196 \mu\text{mol h}^{-1} \text{g}_{\text{cat}}^{-1}$ was observed under natural sunlight, which was comparable to the value obtained from a solar simulator, but lower than that from a UV-A system (as shown in the Table 1). The composition and intensity of irradiating light, however, were different between the solar simulator and natural sunlight systems. The UV light was removed by a UV filter for the solar simulator system (25 mW cm^{-2}), while UV light was present in the natural sunlight system, which was reported to have an average solar power of 2.5 mW cm^{-2} for the UV range and 45 mW cm^{-2} for the visible range. Simultaneous production of H₂ and liquid phase compounds (e.g., sugars and organic acids) was monitored under direct solar irradiation (St Andrews, Scotland, UK, July, temperature 16 °C) in an aqueous solution containing cellulose@Pt/TiO₂ (i.e., Pt/TiO₂ photocatalyst coated by cellulose) [29]. The authors reported a $r_{\text{H}_2} = 27 \mu\text{mol h}^{-1} \text{g}_{\text{cat}}^{-1}$, which despite being lower than that achieved with a 250 W UV lamp ($933 \mu\text{mol h}^{-1} \text{g}_{\text{cat}}^{-1}$), demonstrated the feasibility of using natural sunlight for generating H₂ from photo-reforming of lignocellulosic materials. It should be noted, however, that the efficiency of photocatalytic reactions (i.e., AQY or STH) under natural sunlight and artificial irradiation is challenging to compare as the light intensity reaching the catalyst, which dictates the photocatalytic activity, could be heavily influenced by photoreactor geometry and engineering. Parameters such as overall configuration, materials, reactor volume, active photocatalyst surface area, mass transport and light distribution are crucial for facilitating an enhanced reaction. Previous studies have considered reactor engineering for photocatalytic H₂ generation including investigating fluidisation approaches [20, 59], technical and economic feasibility [60] and more recently the deployment of large-scale (100 m^2) solar photocatalytic water splitting units [61, 62]. To date, however, there have been no reports in the literature which have focussed on reactor design exclusively for photocatalytic biomass reforming.

2.2 Photocatalytic Reforming of Lignin and Lignin Models

To date, the majority of biomass photocatalysis research has focused on cellulose (and/or other carbohydrates) as a model compound where, in addition to the production of H_2 , valuable chemicals can also be formed. The most abundant compounds from cellulose photo-reforming are monosaccharides (such as glucose and arabinose) and HMF [29, 45–48] with cleavage of the β -1,4-glycosidic bond regarded as the key step in the process [30, 65, 66, 69]. Lignin, however, makes up a large portion of raw biomass and is considered the more unreactive and recalcitrant constituent of the native material. Its chemical composition represents a challenge for biomass conversion processes and as a result is often underutilised. Despite this, targeted degradation of lignin has the potential to yield various chemicals of potential interest to the fine chemical industry [70] and which have been produced alongside the production of H_2 in several systems.

In terms of the formation of both an energy vector and valuable products from lignin-based feedstocks, several studies have been reported in the literature. Zhao et al. performed photo-reforming of Kraft lignin in 1 M NaOH solution with a TiO_2 -NiO n-p heterojunction catalyst to yield both H_2 and CH_4 as the gas phase products along with the generation of fatty acids in the liquid phase [49]. These compounds included palmitic (35%), stearic (25%) and butanedioic acid (7%), which are capable of being further converted into biofuels. In this study, the n-p heterojunction of the TiO_2 -NiO catalyst was shown to be effective in separating and migrating the electron-hole pair which facilitated the redox reactions at the catalyst surface. While electrons formed on the TiO_2 surface led to the formation of H_2 , photogenerated holes facilitated the oxidation of lignin to form the acids [49]. Work conducted by Kadam et al. demonstrated that the photo-reforming of the sodium salt of lignosulfonate using C-, N- and S-doped ZnO catalysts was capable of producing both H_2 and the primary product 1-phenyl-3-buten-1-ol. The authors proposed H^+ to be the active species in the photo-oxidation of lignin via direct oxidation at the catalyst surface [68]. Sun et al. [71] studied the photocatalytic cleavage of lignin model compound 2-phenoxy-1-phenylethanol using a Ni/CdS catalyst in various solvents, which were shown to influence the rate and product distribution. The lignin substrate was oxidised to a ketone product (2-phenoxy-1-phenylethanone), which was concurrent with H_2 generation occurring at the conduction band. The reactions were conducted in pure CH_3CN and irradiated for a period of 18 h from an 8 W blue LED (wavelength range = 440–460 nm). The authors reported that the selectivity and conversion of the reaction achieved was ~100%. In comparison, by using a CH_3CN/H_2O (20:80) solution, the study found that the lignin model compound was converted within 8 h of irradiation, and acetophenone and phenol, along with 2-phenoxy-1-phenylethanone, were the photo-oxidation products formed. Furthermore, in alkaline conditions, (i.e. $CH_3CN/0.1$ M KOH) full conversion of the lignin substrate was achieved in 3 h of light irradiation with more than 90% acetophenone and phenol formation. It was expected that the H^+ in Ni/CdS was responsible for the oxidation of the $C\alpha$ -OH group in 2-phenoxy-1-phenylethanol, resulting in the generation of 2-phenoxy-1-phenylethanone as the primary product. Meanwhile, H_2 was produced utilising the proton extracted from the 2-phenoxy-1-phenylethanol.

Photo-oxidation for the generation of aromatic compounds from lignins has been more widely studied than the systems described above, which produced both H_2 and value-added compounds. Selective formation of desired products is however, still a significant challenge for photocatalytic reforming of biomass to chemicals due to unselective oxidation reactions and the complexity of lignin substrates (insolubility and low reactivity). One strategy to improve the interaction of lignin with the catalyst included wet-milling of lignin and TiO_2 prior to photo-oxidation which resulted in increased depolymerisation to phenolics [72]. An alternative strategy outlined in the study by Wu et al., improved catalyst-substrate interaction through solubilising the catalyst as opposed to lignin. The solubilisation and dispersion of the catalyst in an aqueous methanolic solution, and functionalisation of CdS QDs with 3-mercaptopropionic acid improved the interaction of the catalyst with native lignin [73]. The authors stated that the colloidal CdS QDs were utilised in a 'lignin-first' visible light-activated conversion of biomass (birch woodmeal), to monomeric aromatics (~27% yield) which proceeded without conversion of cellulose or hemicellulose [73]. Interestingly, following separation of the catalyst, cellulose and hemicellulose fractions could be recovered for acidolysis/enzymatic hydrolysis to form xylose and glucose. The CdS catalyst in this study was reported to activate the dominant linkage in lignin, the β -O-4 bond, which was subsequently cleaved by an electron-hole coupled photoredox mechanism.

While the use of raw biomass and lignins represents a clear step forward for photocatalytic reforming of biomass, it also highlights the need for fundamental research into the effect of the technology on different lignin bonding patterns. As such, there is research which has focused on exploring the impact photocatalysis can have on the lignin structure through deploying model compounds which contain the key linkages found in the native material, e.g., β -O-4 [74–79], β -5 [80] and 5–5' [81] linkages. The proportion of these bonding patterns varies within lignin; however, in softwood species the relative proportions of β -O-4, β -5 and 5–5' biphenyl are 45–50, 9–12 and 19–22%, respectively [82]. The structure of lignin is shown in Fig. 5, which highlights the range of bonding patterns present in the material.

Model compounds containing the β -O-4 linkage have been the most reported in the literature, which is because the linkage is the most abundant in native lignin and the relative simplicity of synthesising the materials. An overview of the transformation detailed in the literature is shown in Fig. 6. Work by Stephenson et al. demonstrated that photo-redox catalysis was capable of degrading lignin model compounds containing a β -O-4 linkage [76, 77]. The group developed a dual-catalytic system whereby photo-redox was followed by a co-catalytic system of palladium in the presence of sodium persulfate as a terminal oxidant. An octahedral iridium complex as a photocatalyst along with palladium catalysis could undergo a single electron transfer to perform an α -oxidation thus weakening the adjacent bonds in the linkage. The use of the dual-catalytic strategy allowed for the oxidation of both primary and secondary alcohols within the β -O-4 model compound, followed by fragmentation via C–O and C–C bond cleavage.

A combined approach was also adopted by both Wang et al. [78] and Zhang et al. [83]. The former utilised photocatalytic oxidation with hydrogenolysis in a dual-light wavelength switching strategy, while the latter utilised electrochemical

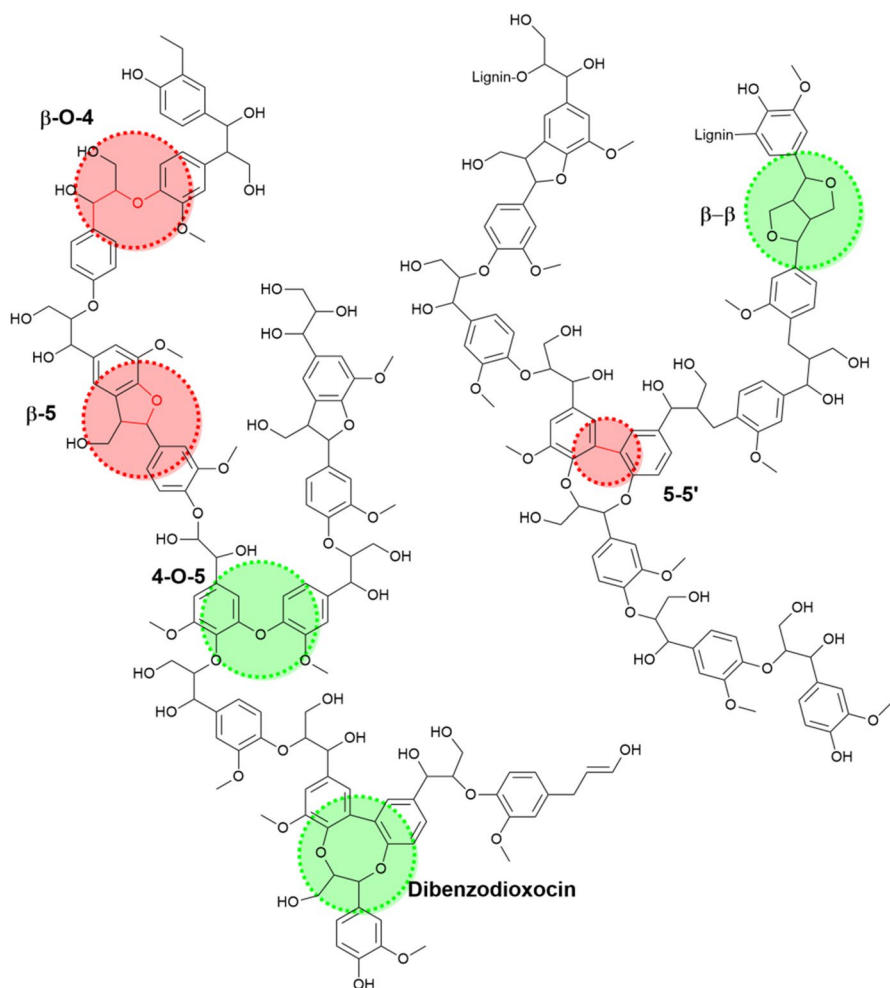


Fig. 5 Structure of lignin identifying the key linkages including the β -O-4, β -5 and 5-5' biphenyl bonding patterns (in red)

oxidation followed by photocatalytic C-O bond cleavage. The work by Wang et al. demonstrated that β -C-O bonds can be cleaved in β -O-4 model compounds, with the authors proposing that a radical driven process produced two fragments of the β -O-4 model compound. In the work by Zhang et al., the rationale behind this approach was supported by previous calculations by Beckham et al. [84], whereby it was shown that oxidation of a benzylic alcohol (to provide the carbonyl) weakened the β -C-O bond by as much as $13.3 \text{ kcal mol}^{-1}$. The dual strategy meant that once this bond was effectively weakened due to the oxidation process, the photocatalytic cleavage of this bond was more favourable.

In contrast to the β -O-4 linkage, research on the photocatalysis of model compounds containing the β -5 and the 5-5' biphenyl linkages have been limited. While

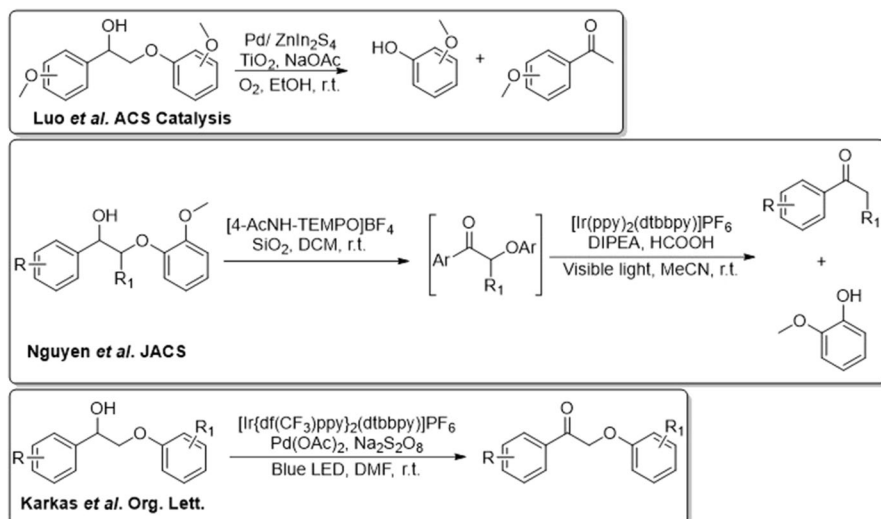


Fig. 6 Transformations employed for the conversion of β -O-4 model compounds. Information shown in the figure is reprinted (and adapted) with permission from [76–78]. Copyright 2022, American Chemical Society

there are several studies detailing syntheses of the compounds [85–88], work on their degradation is not frequently reported. Castellan et al. [89] showed that by using the biphenyl models divanillin and divanillyl alcohol, degradation can be achieved using TiO_2 photocatalysis in an ethanol–water solvent mixture.

Similarly, research associated with β -5 linkage has typically focused on synthesis, as opposed to photocatalytic conversion. Recently, Murnaghan and coworkers demonstrated the use of TiO_2 in the photocatalytic degradation of a β -5 model dimer [80]. Under low power (~ 1 W) UV-LED irradiation, complete degradation of the β -5 compound was achieved along with formation and subsequent removal of reaction intermediates. Murnaghan et al. [90] observed the generation of a diol species within 2 mins of irradiation which was determined as the initial step in the conversion of the dimer. Subsequently, further bond cleavage resulted in the formation of several key reaction intermediates, Fig. 7.

3 Future Perspective for Photocatalytic Reforming of Biomass

Providing a future perspective on photocatalytic reforming of biomass is challenging, especially considering it is a research topic which is still relatively new. Part of providing that perspective comes from identifying the current technology status along with the target status and reviewing the challenges that separate those two points. Beyond that, however, it is crucial to explore the additional parameters which can influence technology development, and in particular the ‘incentive’ which can drive this, e.g., industrial engagement. This section addresses these points in more

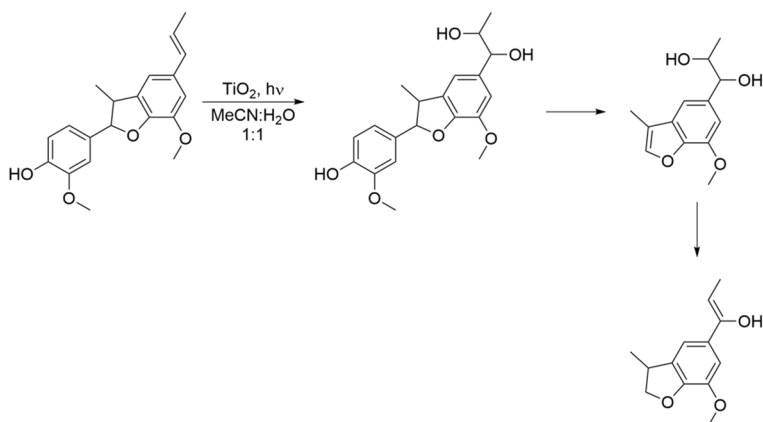


Fig. 7 Scheme of events leading to the products found in the TiO_2 -mediated photocatalytic degradation of a β -5 model compound [90]

detail by adopting a holistic view of photocatalysis as a process and technology for the conversion of biomass to energy.

3.1 Assessing the TRL of Biomass Photocatalysis

The use of a simple 1–9 scale, which is accompanied by a clear description for each position, allows the TRL scale to become an extremely valuable tool for assessing emerging technologies such as photocatalysis. The diverse range of applications photocatalysis has been applied to has resulted in the technology covering the entire TRL scale. While a TRL of 9 indicates a mature technology that has been deployed at scale, there are few examples of photocatalytic processes achieving this, with self-cleaning the most notable [91, 92]. In contrast, most applications remain within a TRL range of 1–6 with environmental remediation considered the more developed process when compared to alternatives such as chemical synthesis and energy production, Fig. 8.

The TRL position of photocatalytic processes can often reflect the chemical complexity and challenges associated with these applications. The non-selective nature of ROS facilitates the removal of contaminants from air and water more effectively than they do for the generation of an energy vector (e.g., H_2) or desirable bioproduct (e.g., value-added compounds). Moreover, the presence of competing reactions such as electron scavenging, and reaction product oxidation can further reduce the potential feasibility of the process. Subsequently, the TRL position of photocatalytic reforming of biomass can be seen in Fig. 9, where it is positioned between 1–3. If the primary applications are considered as H_2 generation, bioproduct formation and combined systems (e.g., simultaneous energy and value-added compounds), additional subcategories can also be included on the TRL scale. A key factor when assessing the TRL status of any technology, is the requirement that the conditions of a certain level (e.g., TRL 5) are achieved or demonstrated for a technology to be

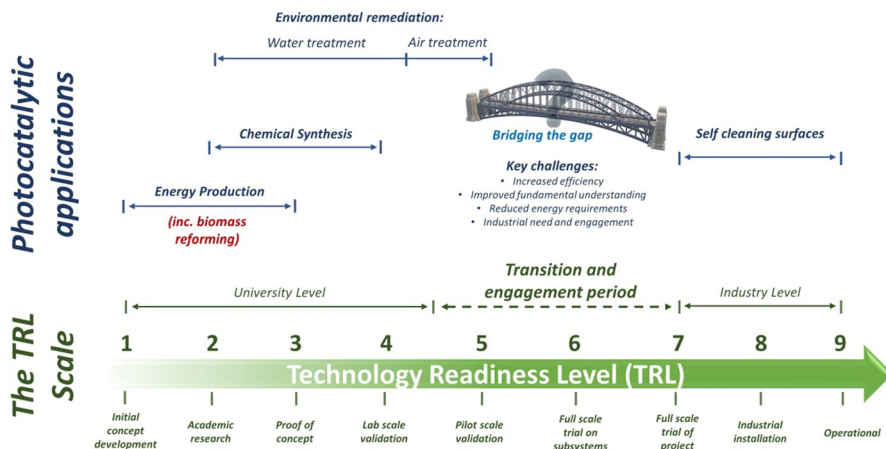


Fig. 8 An overview of the TRL scale for photocatalytic applications. Adapted from [34] with kind permission from Elsevier

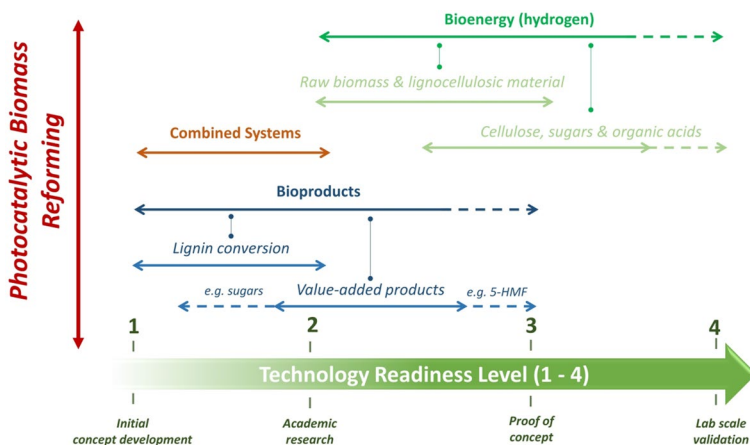


Fig. 9 The TRL scale in relation to photocatalytic biomass reforming, where solid lines represent the current range for specific applications and the dashed lines represent potential for expansion (based on recent or related literature)

considered at that level. For instance, a technology at TRL 5 does not progress to 6 simply by achieving the criteria of 5—it must demonstrate the requirements of TRL 6 first. Therefore, this allows photocatalysis technologies to be viewed in relation to both what has been achieved and what must still be achieved to further develop. As Fig. 9 highlights, H₂ generation can be considered the more advanced technology within biomass photocatalysis with a TRL of 3. Interestingly, this value can vary if the subsections of feedstock are considered; raw biomass (e.g., lignocellulose and/or only lignin) is still at the proof-of-concept stage (TRL 1–2) while alternative feedstocks (e.g., sugars or organic acids) are supported by more substantial laboratory

data and as such are approaching lab scale validation. The latter is likely a result of sugars and organic acids being utilised as SEDs for H₂ generation for several years prior to photocatalysis being deployed as a method for biomass conversion. Moreover, if biomass is considered as a (more cost effective) SED, photo-reforming to H₂ can also build on the extensive research conducted into photocatalytic water-splitting and H₂ generation (from other SEDs). This may also include examples of larger scale solar photocatalytic H₂ generation, and more recently the solar water splitting photoreactors in Japan [61, 93, 94]

In contrast, bioproduct generation and combined systems have a TRL of 1–2, as research in this area is still in its infancy. As highlighted in the Figure, subsections for these topics include lignin (and lignin model) conversion and value-added product formation, identifying HMF and sugars as example target compounds. A potential limiting factor within this area is selectivity of products and overall yield, which has resulted in literature focusing more on H₂ generation. It is worth noting, however, that research into value-added compounds can be more focussed on the fundamental chemistry associated with the mechanisms, e.g., the use of lignin models to identify which linkages are cleaved during the reactions. While TRL advancement in this area may be restricted, the work could be highly complementary to enhancing the understanding of how H₂ is formed, which in turn would facilitate the development of that application towards a higher TRL. The source of protons in biomass photocatalysis processes remains relatively unknown due to the presence of multiple reaction intermediates in the oxidation pathway. An improved understanding of that could be utilised to increase the concentration of protons available at the catalyst surface for accelerated H₂ production.

Therefore, by adopting a more holistic evaluation of the technology through tools such as the TRL scale, the interdependency of these applications can be demonstrated. Interestingly, there is evidence of this approach now being adopted within recent literature for the application of waste photo-reforming. Rumayor et al. performed a life cycle analysis (LCA) on the photocatalytic reforming of waste (e.g., glycerol) for H₂ generation with a view towards evaluating the environmental impact and potential feasibility of such a system [95]. Their approach used both water electrolysis and SMR (i.e., green and grey/blue H₂, respectively) as benchmarks in the study to ascertain the validity of photocatalytic technology for sustainable H₂ production in the future. The investigation considered two possible reactor configurations based on the method of irradiation: artificial with LEDs and direct solar via a compact parabolic collector (CPC), Fig. 10. The work considered several operational scenarios and while it demonstrated the challenge in conducting this type of research, especially for an emerging technology, it also underpinned the significant potential photocatalysis technology has moving forward. This was demonstrated in relation to global warming potential (GWP), which identified direct solar irradiation (e.g., Sc. 2-PV-Solar and Sc. 2-Wind) as having the lowest potential GWP at <0.4 kg CO₂-eq (Fig. 11). Under scenario 2 (Sc. 2) renewable energy was utilised only for mixing and stirring as opposed to Sc. 1 which utilised renewable energy for mixing, stirring and the LED irradiation array. The authors concluded that even

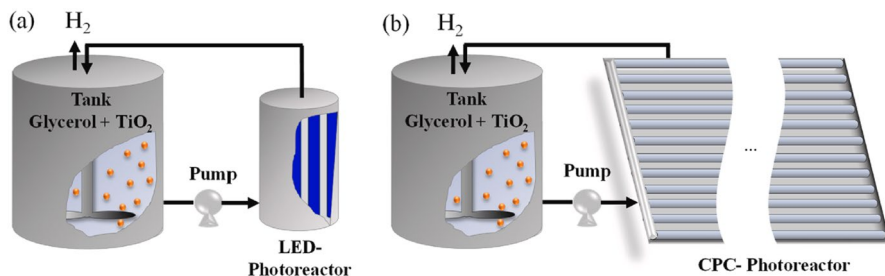
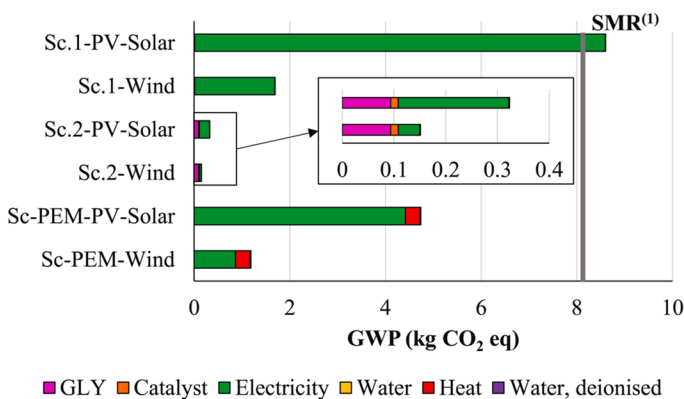


Fig. 10 Reactor configurations considered in the work by Rumayor et al. [95] for the photo-reforming of glycerol to H₂, where (a) consists of a LED photoreactor and (b) consists of a CPC-photoreactor. Image reprinted with kind permission from Elsevier



⁽¹⁾ GWP impact obtained from GaBi database.

Fig. 11 The results of the LCA conducted by Rumayor et al. [95] in relation to Global Warming Potential (GWP) of different photocatalytic glycerol reforming scenarios (Sc) and reference scenarios for polymer electrolyte membrane (PEM) electrolyzers. Sc-PEM per functional unit (1 kg of H₂). Image reprinted with kind permission from Elsevier

under low production rate conditions (e.g., $\sim 5 \times 10^{-4}$ kg H₂ hr⁻¹), photocatalytic technology in both scenarios could provide green H₂ with a GWP that was comparable to other renewable driven processes, e.g., water electrolysis. While that statement alone is a substantial observation within the context of photocatalysis research, it is crucial to consider two additional points. This paper is one of the first to attempt an LCA-based study of photocatalytic H₂ generation, which is a potential indication of the status the technology is reaching. Secondly, the scenarios presented in the study were, as the authors stated, ‘a simplification of a complex reality’. Therefore, it is paramount that studies such as this one be utilised in conjunction with identifying and addressing the additional challenges which are present in this area.

3.2 Identifying Challenges

The challenges associated with any photocatalytic process can often be viewed under the core headings of catalyst (including the reaction kinetics), reactor, and lights. These can also be applied to photocatalytic biomass conversion; however, it is important to note that there are specific challenges within this topic that are not associated with processes such as water splitting and/or CO₂ reduction. In evaluating such a system, it is important to understand from the outset what would be regarded as a realistic target for an efficient process. This can be assessed with respect to the nature of the biomass feedstock, what the target products are, what yields are achievable for these products and what the overall efficiency of the process is in achieving these yields.

With respect to the photocatalyst and the reaction (e.g., substrate conversion), the nature of the feedstock will be a critical initial consideration. As discussed in Sect. 2, the photocatalytic reforming of a range of different biomass feedstocks has been reported in the literature ranging from refined cellulose through to grass. Each of these feedstocks presents challenges in terms of effective deployment and distribution of the material relative to the photocatalyst. The presence of biomass as a suspended solid within a photocatalytic reactor limits catalyst-substrate interaction and as a result can inhibit the effectiveness of ROS. This can also be coupled with the recalcitrant nature of biomass which again can present a challenge for ROS, especially if bond cleavage (e.g., lignin linkages and glycosidic bonds) is not achieved. Therefore, depending on the feedstock there may be a requirement for either chemical or physical pre-treatment prior to deployment in a photocatalytic reactor. The inclusion of such a step may influence the overall viability of a scaled system, much in the same way as filtration (or additional downstream processing) does for a TiO₂ slurry reactor. The financial and energy costs of such processes must be considered when assessing the overall efficiency. A final consideration for biomass conversion technologies is the source (i.e., imported, nationally distributed or locally sourced) and availability (i.e., quantity and consistency of supply) of the biomass feedstock itself. There is little point in developing a system for biomass resources which are in limited supply or varied purity and/or form which would necessitate re-engineering of the reactor and catalyst setup to ensure a practical product yield.

Additional points related to the photocatalyst include both the yield of product generated and under what irradiation source. As previously highlighted, the product yields of both H₂ and chemicals, such as carbohydrates, generated from the photocatalytic valorisation of biomass are still low—typically in the micromolar scale after several hours of irradiation. This is significantly lower than the litre or cubic metre scale that would be required for a practical system even at a prototype level. The challenge in increasing the scale of product yields and efficiency of the process will depend on several factors, particularly the photocatalyst material itself. This is further influenced by the electronic structure of the catalyst and its potential for visible (or solar) light activation. Due to the lower attenuation of visible light compared to UV through fluids and also the potential for utilising solar light, a visible-light active photocatalyst would be highly desirable for photocatalytic valorisation of biomass. Since the late 1990s there have been extensive reports of visible-light active

photocatalyst material for both water treatment and energy conversion applications, which have often had variable efficiencies. Even if an effective photocatalyst material which can generate molar quantities of products (or even cubic metre levels per hour) was generated, that material will need to be viable for commercial scale production. With the exception of a modified TiO₂ material, produced by Kronos, no visible light-active materials are currently available commercially. For any process to be practical on a large scale, photocatalyst materials will need to be available in kilogram/tonne quantities. Consequently, for any potential upscaling, at the moment, a commercially available photocatalytic material (such as Evonik TiO₂) would need to be utilised as the photocatalyst. While this material is available in bulk quantities, it still requires UV light (~385 nm) to activate it.

Moving beyond the challenges of catalyst development, the method of deployment becomes paramount. This includes the role the reactor plays in maximising the active photocatalyst surface area, light intensity and distribution, mass transport and product separation. In terms of the scope of this article, it is not possible to go into all the specific engineering challenges in depth, and to do so would be the subject of a detailed article in itself. The issues raised here, however, are some of the key issues that would be considered the most significant challenges for a biomass-based system and those that would need to be addressed in developing a prototype or small-scale units before considering larger scale systems. The reader is directed towards several excellent papers that review and investigate the specific details of photoreactor concepts [96–100].

Within photoreactor design, reduced mass transfer and enhanced light distribution are two parameters which present a challenge when considering biomass feedstocks. Ensuring effective mass transport in photocatalytic reactors is often challenging, and this is further increased in the conversion of biomass due to the recalcitrant and insoluble nature of the material. Moreover, the presence of suspended biomass particles within both flow and batch reactors can also impact the rate of conversion. Therefore, providing an active catalyst is deployed (as either a suspension or immobilised onto a support), it is crucial the reactor can maximise the interaction between the suspended feedstock and catalyst surface. While this point has not been exclusively addressed in the literature for this topic, it has been an issue when investigating reactor engineering characteristics for other photocatalytic processes [101–104]. Several approaches have been previously adopted in photocatalytic treatments systems including the use of enhanced flow systems and agitation via mixing or sparging with air/oxygen, application of rotating disc reactors and use of turbulence promoters such as baffles [20, 105–108].

In addition to mass transfer limitations, effective distribution of photons within a photoreactor becomes challenging because biomass feedstocks are capable of absorbing and scattering light. Moreover, the turbidity created from a biomass suspension can also reduce light penetration and subsequently limit photon absorption at the catalyst surface. Even when the method for determining irradiation intensity in a photocatalytic reactor is clear, how the light is distributed within that reactor and how much is actually involved in the process is not always apparent. Understanding this, however, is crucial as it provides a platform to then assess the potential impact of biomass within the reactor. Meng et al. (2019) discussed how the radiation

transport equation (RTE) can be used to model light intensity distribution on photocatalytic reactors [109]. The light intensity as a stream of photons that moves through the photocatalytic reactor will depend on the following parameters: absorption of light, out-scattering of light and in-scattering of light. The out-scattering of light occurs when light is scattered out of the light path and is, therefore, deemed not to be available for interaction with photoactive materials. In contrast, in-scattering refers to light that is scattered back into the light path and hence is available for interaction with photoactive materials. The RTE for a photocatalytic reactor is a combination of the absorption, out-scattering and in-scattering terms (Eq. 1) [109].

$$\frac{dI_v(s, \Omega)}{ds} = \underbrace{-\kappa_v I_v(s, \Omega)}_{\text{Absorbed light}} - \underbrace{\sigma_v I_v(s, \Omega)}_{\text{out - scattered light}} + \underbrace{\frac{1}{4\pi} \sigma_v \int_{4\pi} p(\Omega' \rightarrow \Omega) I_p(s, \Omega') d\Omega'}_{\text{In - scattered light}} \quad (1)$$

where $I_v(s, \Omega)$ is the monochromatic light intensity along the path s in the direction Ω , κ_v is the coefficient of absorption, σ_v is the coefficient of out-scattering, Ω is the direction of the light stream, Ω' is the direction of light from other directions and $p(\Omega' \rightarrow \Omega)$ is the phase function of in-scattered incident irradiation to an element from other directions (Ω') [109].

This equation highlights the complication with biomass photocatalysis as the material itself is likely to both absorb and scatter light and hence limit the intensity reaching the surface of the photocatalyst material. This will clearly have an impact on overall efficiency of the process but in particular the quantum/photonic efficiency. Under such conditions, ensuring that light can be effectively delivered to the surface of the photocatalyst in the presence of a complex biomass material is not simple. As a result, this becomes a challenge that must be addressed by reactor engineering in view of the geometry between catalyst deployment and irradiation source array. The immobilisation of the photocatalyst to a substrate which allows direct catalyst irradiation (e.g., irradiation through a transparent support or via an optical fibre coated with a photocatalyst) rather than through the biomass matrix could aid this process. The limitation to this approach, however, is that the relative active photocatalyst surface area will be reduced if compared to that achieved for a suspended catalyst system with a similar footprint.

Finally, an important aspect of developing photocatalytic systems for biomass conversion is the metric which is used to assess activity. Assuming an active catalyst is effectively deployed in a suitable reactor which can utilise a range of biomass-based feedstocks, the metric by which that activity is measured becomes a crucial consideration. As with other photocatalytic processes, selection of an appropriate measure of efficiency is an issue, as there is often inconsistency in how this is reported between different laboratories. Many groups report efficiencies of processes in terms of yields of products by the photocatalyst (e.g., $\mu\text{mol h}^{-1} \text{g}_{\text{cat}}^{-1}$), while others report the quantum (or formal quantum) efficiencies based on the ratio between the reaction rate and number of photons (which is often represented as an intensity). While such measures are appropriate for photochemical/catalytic processes, they are less informative for more whole-system comparisons. This point also highlights

another key challenge within photocatalysis which is associated with the lack of standardised testing to provide a more accurate platform for comparison. The use of an appropriate metric could be extremely valuable for encouraging engagement with potential industry stakeholders. While a photonic efficiency is useful at lab scale, it offers a limited insight into the performance of the entire system, which is what would be required to demonstrate pilot scale feasibility.

3.3 Roadmap for Technology Deployment

The previous sections highlighted the technology status of photocatalytic reforming of biomass along with the challenges associated with advancing the field. While these challenges are significant and require dedicated research to address and potentially overcome them, the deployment strategy for photocatalytic technology can also influence the research conducted with a view towards establishing a roadmap. The literature has often stated the main objective for photocatalysis as being towards industry level operation and deployment, and while that will always remain as the core objective, examples of this being achieved are very limited. This point was also discussed in the excellent work by Loeb et al. when they reviewed the technology horizon for photocatalytic water treatment, specifically identifying that ‘technology transfer problems’ are being overlooked which widens the gap between research and industry [110]. As discussed by Loeb and colleagues in their feature article, this issue is somewhat reflected in literature trends; of the 1356 papers published on photocatalytic water treatment in 2017, only 29 contained the term ‘pilot’. Given the TRL status of that application, a higher proportion of industry-facing research would be expected. Their literature review, however, suggests topics such as reactor design and pilot-scale studies are not as routinely investigated as those on reaction kinetics and material synthesis.

In comparison to photocatalytic biomass conversion, the issues surrounding technology transfer barriers are further emphasised, primarily due to the maturity of the application. With that being said, there is justification for the argument that the research in this field is simply at too early a stage to be considering a roadmap or deployment strategy. There is, however, evidence in recent literature that highlights a potential transition towards process design for solar-to-H₂ technologies being more prominent. In 2021, the largest to-date solar H₂ production unit of 100 m² was reported by Nishiyama et al., which was composed of panel reactor arrays with SrTiO₃:Al as the photocatalyst [61]. In addition, the rapid growth of this field is demonstrated by Fig. 12, which also highlights the research trends emerging within the literature. Despite the first publication on this topic being in 1981, it was not until 2010 that a more substantial increase in the number of publications was observed. This was subsequently followed by a significant increase from 2014 onwards, with 315 papers published last year (2021) which contained the keywords ‘photocatal*’ and ‘biomass’. Interestingly, if the literature search is extended to include sub-topics associated with the field, as shown in the Fig. 12 insert, then ‘hydrogen’ and ‘visible’ are clearly the most active research areas accounting for ~47 and 44% of the total, respectively (in 2021). It should be noted that the number of publications

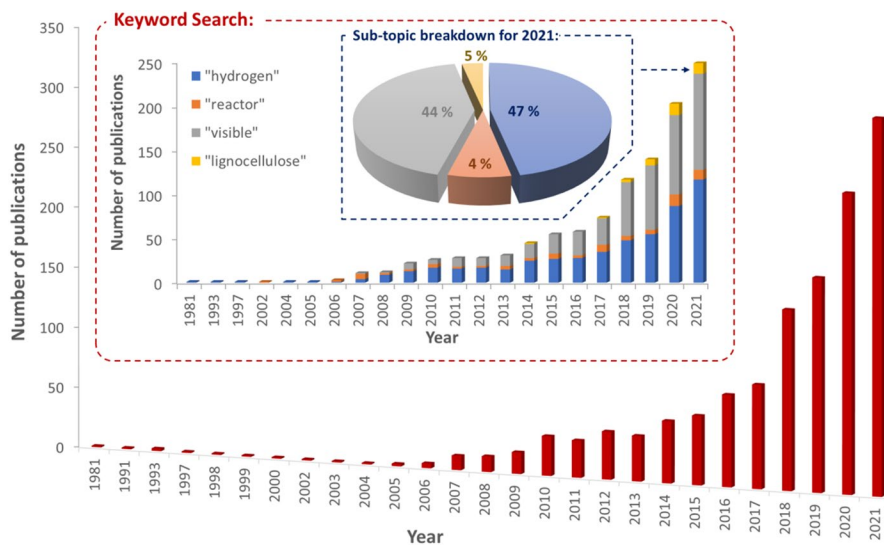


Fig. 12 Literature trends for publications on photocatalysis biomass research. The main graph shows the number of publications from a Web of Science search using the keywords ‘photocatal*’ and ‘biomass’ during 1981–2021. The Keyword Search insert provides a further breakdown of the literature trends during the same period based on additional keywords of ‘hydrogen’, ‘reactor’, ‘visible’ and ‘lignocellulose’, while the sub-topic breakdown for the 2021 insert shows the percentage of papers published in 2021 that contained those same keywords

including the term ‘lignocellulose’ has also increased since 2017 suggesting that the use of raw biomass as a substrate is increasing. Figure 12 also shows that despite an increase, reactor-focussed research remains less prominent than other sub-topics within this field, accounting for only 4% of the total. In relation to addressing potential technology transfer barriers, this may pose a challenge as research continues to focus and develop around materials and not entire systems. These topics are not independent of course, and it is to be expected that, at this stage, research will (and needs to) focus on catalyst enhancement for use with raw biomass. It is crucial, however, that there is an awareness of how these more-active research areas can encourage and facilitate the growth of associated topics such as reactor engineering and whole-systems analysis.

As indicated by the previous TRL scale (Fig. 8) and by Loeb et al. [110], photocatalysis has been shown to struggle when attempting to overcome technology barriers such as pilot-scale validation, large-scale trials and industrial engagement. There can be several contributing factors to this; however, a lack of clearly identified research priorities could be crucial. In the work by Loeb et al., a series of recommendations were made that provided a framework for advancing the field of photocatalytic water treatment towards higher TRL status and integration into existing industry infrastructure. A similar approach can be applied here, despite the application of photocatalytic biomass conversion being at a lower TRL than water treatment, TRL = 3 and 6, respectively, for biomass reforming and environmental remediation. In doing so, it could allow for research priorities to be identified sooner which would ensure

that technology transfer barriers are considered alongside fundamental research as opposed to during later stages. Furthermore, there is additional incentive for technology development that is not often considered or associated within other photocatalytic applications. NZE targets and with it, renewable energy strategies, have significantly altered the future energy landscape and rapidly put focus on a range of current and emerging methods that can contribute towards both. While this is applicable to multiple photocatalytic applications, topics such as biomass (and/or waste) conversion and CO₂ reduction are at the forefront.

Therefore, what does a roadmap for technology development in photocatalytic biomass conversion look like? Answering this question is subject to several factors; however, it can be aided by considering a potential future deployment scenario for photocatalytic biomass conversion technology to produce H₂. In any biomass conversion technology, the scale of the production and utilisation of H₂ as an energy vector (or as a chemical feedstock itself), requires consideration in development of a process. For any biomass-to-H₂ technology, the production/utilisation of H₂ could be considered as either:

1. a centralised biomass-to-H₂ process with distribution of the H₂, for example, integration into the current natural gas infrastructure or
2. as a localised production process with the biomass resource available on the same site as H₂ production and utilisation.

In any biomass-to-H₂ process, the availability of the biomass at the scale required for the process is a key consideration. The potentially large scale of H₂ production required in a centralised–distributed deployment scenario could see blue H₂ dominate within this strategy in the short to medium term as the feasibility of green H₂ production from electrolytic water splitting is investigated, for example, through pilot H₂-to-homes schemes such as Fife H100 [111]. It is, however, within a localised production scenario, where emerging renewable driven H₂ technologies could be envisaged to play a more significant role.

In the scenario of photo-reforming of biomass for the localised production of H₂, whilst removal of the biomass transportation costs would provide financial and environmental benefits, the scale of the H₂ production would still need to reflect the availability of the biomass resource. A scenario could be envisaged where biomass feedstocks, such as energy crops (miscanthus or willow) or wastes from agriculture/forestry could be used in a photo-reforming process activated by sunlight and/or wind-powered LEDs, Fig. 13. The generated H₂ could be a feed for fuel cells generating electricity which could be used on site (remote locations) or connected to the national grid. Such a scenario requires consideration of the scale and technical specifications of the respective feedstocks for H₂ production (biomass/water) and utilisation (gas purity/separation) processes but direct use of the H₂ produced could remove H₂ storage requirements providing further (financial) advantages for small-scale localised applications.

It is worth noting that the H₂ (produced from photo-reforming) could be used as a feedstock for production of fuels such as methanol or ammonia or coupled

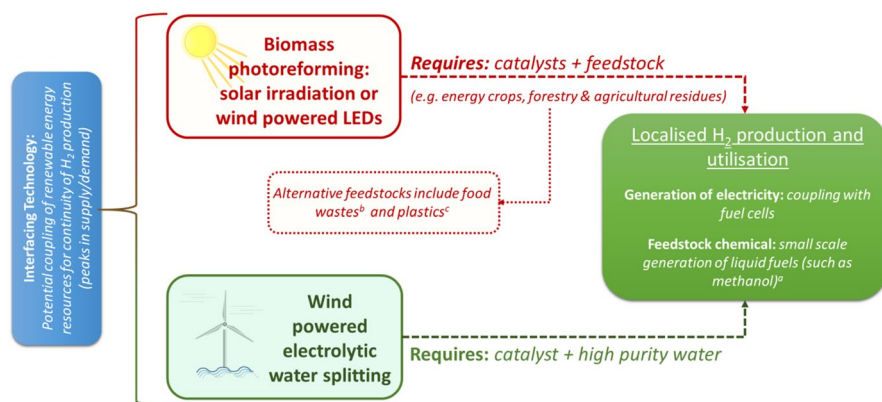


Fig. 13 Illustration of a potential deployment scenario for photocatalytic biomass reforming based on a range of feedstocks for H_2 production and utilisation in electricity generation and/or as a feedstock chemical. References within the figure include [112]^a, [113]^b and [114]^c

with emerging mild catalytic processes (not requiring pressurised H_2), e.g., the non-thermal plasma catalytic hydrogenation of CO_2 and reverse water gas shift under ambient conditions [115–117]. If the H_2 consumption rate by the catalytic system (fuel cell/plasma reactor) can be matched by the H_2 production rate from a photo-reforming process, the renewable H_2 produced can be used locally and immediately for production of electricity or relevant platform chemicals such as CH_4 and CO .

Perhaps a logical question in relation to the above discussion is what would a proposed reactor design be for such a deployment scenario? Literature on reactor design for photocatalytic H_2 generation, especially utilising biomass, is scarce, however, which presents a challenge when attempting to forecast what would be required. Currently, the most viable approach would be to recommend desirable design parameters that should be researched in tandem with the design and optimisation of catalysts. As such, two key factors are irradiation, including delivery and distribution, and catalyst deployment which considers immobilised and suspended systems. As discussed, utilising solar energy remains the primary target for irradiation, and where possible reactors should enhance distribution within units to maximise photon absorption at the catalyst surface. Where solar is not suitable, artificial arrays comprising LEDs are highly desirable, providing they are coupled with renewable energy such as wind. Catalyst deployment, however, is a more significant challenge that covers both chemistry and engineering. A catalyst immobilised onto a stationary support can alleviate the downstream processing requirements often associated with suspended systems. A drawback, however, is overcoming the mass transfer limitations which could be significant in a biomass-based photocatalytic system as the feedstock is likely to have low solubility. While not biomass-focussed, two different photocatalytic reactor systems for H_2 generation from water splitting, namely particle suspensions and planar arrays, were designed and compared by Pinaud et al.

[60]. The particle suspension system was an enclosed aqueous reactor bed of suspended photoactive particles, while the system of planar arrays consisted of multi-layer absorber planar arrays immersed in an aqueous electrolyte and oriented toward the sun. To compare them, the STH conversion efficiency of each system was estimated, and the results showed that the STH efficiency of single and dual bed particle suspension systems was 10 and 5%, respectively, while the value was 10 and 15% for fixed panel array and tracking concentrator array systems, respectively.

In conjunction with considering a future deployment scenario and reactor design for photocatalytic biomass conversion, the metric by which it is assessed is also crucial. If the focus of biomass conversion is on H_2 as a vector (and in lieu of a standardised test) an energy balance approach offers a more appropriate route to determining a system efficiency. Put simply, if more energy is being input into the system than is produced by the H_2 itself, the process is unlikely to be viable in future energy systems. Sathre et al. developed an interesting approach for considering energy balance and life cycle for larger scale photoelectrochemical systems [118]. This elegant modelling approach focussed on three factors:

1. Life cycle primary energy balance
2. Energy return on energy invested
3. Energy payback time.

The life cycle primary energy balance is a measure of the energy provided by the process or system during its lifetime and is calculated using Eq. 2 [118]:

$$\text{Energy Balance} = [TxE_H] - [E_P + (TxE_O) + E_D] \quad (2)$$

where, T is the life of the process/system in years, E_H is the energy in H_2 produced per year, E_P is the energy required to produce the process/system, E_O is the energy required to operate the system per year and E_D is the energy required to decommission the system.

The energy return on energy invested (EROEI) is a measure of the energy that is provided by the system relative to the energy that is input to the system (Eq. 3) [118].

$$\text{EROEI} = \frac{[TxE_H]}{[E_P + (TxE_O) + E_D]} \quad (3)$$

The energy payback time (Eq. 4) [118] considers all energy input and output costs to the system including those associated with decommissioning. This is a measure of the time required for a system to be operated before sufficient H_2 is generated that will balance the energy that was used in both setting up and decommissioning the plant.

$$\text{Energy payback time} = \frac{[E_P + E_D]}{[E_H - E_D]} \quad (4)$$

The approach developed by Sathre et al. could be adopted as a measure of efficiency of the H₂ generation from photocatalytic valorisation of biomass and would give a more appropriate method of evaluating the practical viability of the process a pilot/prototype scale and above [118].

3.4 Strategy for Achieving Deployment

Considering both the current state of the literature and the perspective provided in this article for photocatalytic biomass reforming, the authors have suggested the following points as key for developing a strategy for achieving future deployment:

1. **Catalyst development which facilitates technology growth and not academic hype.** Activity under visible and solar irradiation will remain a primary objective for any photocatalytic application; however, it must be ascertained with due consideration towards additional key parameters. This includes economic and commercial feasibility for large-scale synthesis and deployment, with potential for operation as a thin film or attached to solid support structure. In relation to biomass conversion specifically, the catalyst must be capable of producing a H₂ yield in a millimole range and demonstrate a photonic efficiency of > 50%. Furthermore, a STH efficiency of 5–10% is recommended to realise economically viable solar H₂ production.
2. **Reactor engineering must be elevated to match other key research topics.** While the design of photocatalytic energy-producing systems remains limited, challenges must be addressed now, regardless of the state of catalyst development. These include using existing examples of modular reactor systems (e.g. electrolyzers and fuel cells) to develop modular photocatalytic units which can demonstrate deployment and operation at a range of scales. This must be done with a view towards developing units capable of operating at pilot scale capacity (e.g. 1–5 m³). Alongside this, research on irradiation arrays must move away from lab standards (i.e., Xe arc lamps) and focus on its own twin track approach which includes solar and sustainable artificial irradiation. The former does not simply imply that catalysts are placed under direct solar but instead, that systems are engineered which optimise the distribution, delivery and, where necessary, concentration of solar photons to a catalyst surface. The latter should be centred on the development of LED systems which are capable of utilising low-carbon renewable energy such as wind. Finally, consideration should also be given to how such a system can integrate with both existing infrastructure and/or technology for the delivery of H₂ as an energy vector.
3. **Establish metrics which encourage engagement at both ends of the TRL scale.** The two previous points are significantly enhanced by the development and utilisation of accurate and representative metrics as evaluation tools. While a single value or metric is desirable for such a purpose, it often oversimplifies a complex process or fails to consider all key parameters. As such, a combination of metrics must be adopted by research which provides a more substantial evaluation

of a system. In the first instance, this can continue to be a rH_2 coupled with a photonic efficiency; however, a modified photocatalytic space time yield [119] should also be incorporated, which integrates reaction rates with reactor engineering parameters such as scale and electrical power. Beyond this, metrics must be focused on whole-systems analysis and specifically for photocatalytic reforming of biomass, that includes an energy balance and life cycle approach (as detailed in Eqs. 2–4). Moreover, with a view towards H_2 generation, cost analysis (i.e., \$/kg H_2) and environmental impact (i.e., CO_2 -eq/kg H_2) would provide an indication of performance that is relatable and comparable to current industry standards. It is also crucial that research is conducted to identify these key parameters and more importantly, identify the data sets that are required which allows their determination, e.g., LCA.

4. ***A more even distribution of research priorities and themes is now required.*** While catalyst development will always be a prominent area of research for photocatalysis, it must now make way for more industry-facing topics and themes to improve the overall TRL. This includes the topics discussed in the previous points such as reactor engineering, metric development, and catalyst synthesis and subsequently related topics such as standardised testing. Specifically for photocatalytic reforming of biomass; however, a key research priority is whole-systems analysis through techno-economic analysis (TEA) and LCA. The justification for this is twofold on account of TEA and LCA being able to evaluate and forecast research hot spots. The evaluation of an entire photocatalytic biomass reforming system is extremely valuable in relation to providing accurate metrics which facilitates academic-industrial engagement. Moreover, this approach can also identify where further information is required and, to an extent, identify research priorities. This would include developing an improved life cycle inventory (LCI) for photocatalytic reforming of biomass which would maximise the output of the system analysis.

4 Conclusions

Analysing the literature published on photocatalytic reforming of biomass highlights both the potential of the field and how far the technology still must go to achieve impact. The challenges associated with the latter, however, should not force this application into another academic hype cycle which hinders technology advancement. In contrast, progress to date can be used as a platform to identify key research priorities that can be incorporated into developing a technology roadmap and deployment strategy for photocatalytic biomass reforming. These should include catalyst synthesis for materials that are both solar activated and economically viable for commercial production. In addition, reactor engineering must focus on the design of systems which enhance biomass substrate–catalyst interactions while promoting potential pilot scale deployment. Beyond this, whole-systems analysis (i.e., LCA and TEA) and technology integration (i.e., wind-powered LED arrays) must come to the forefront of photocatalysis research. Moreover, it is crucial that this is accompanied by accurate and representative metrics that act as evaluation tools to

enhance stakeholder engagement across academia and industry. In doing so, the TRL of photocatalytic reforming of biomass can increase and with it, the potential for the technology to be deployed in future energy systems capable of achieving net zero emission targets.

Acknowledgements The UK Catalysis Hub is kindly thanked for resources and support provided via our membership of the UK Catalysis Hub Consortium and funded by EPSRC Grants: EP/R026939/1, EP/R026815/1, EP/R026645/1 and EP/R027129/1. Nathan Skillen and Lan Lan thank the UKRI Supergen Bioenergy Hub 2018, for funding support through Grant number EP/S000771/1. The authors would like to acknowledge King Abdulaziz City for Science and Technology for financial support for Meshal Aljohani's scholarship.

Declarations

Conflict of interest On behalf of all authors, the corresponding author states that there is no conflict of interest.

Open Access This article is licensed under a Creative Commons Attribution 4.0 International License, which permits use, sharing, adaptation, distribution and reproduction in any medium or format, as long as you give appropriate credit to the original author(s) and the source, provide a link to the Creative Commons licence, and indicate if changes were made. The images or other third party material in this article are included in the article's Creative Commons licence, unless indicated otherwise in a credit line to the material. If material is not included in the article's Creative Commons licence and your intended use is not permitted by statutory regulation or exceeds the permitted use, you will need to obtain permission directly from the copyright holder. To view a copy of this licence, visit <http://creativecommons.org/licenses/by/4.0/>.

References

1. UK Government (2020) The ten point plan for a green industrial revolution. London
2. UK Government (2021) Net zero strategy: build back greener. London
3. International Energy Agency (2021) Net Zero by 2050: A roadmap for the global energy sector
4. International Energy Agency (2021) Global hydrogen review 2021
5. Taylor R, Howes J, Cotton E, Raphael E, Kiri P, Liu L, Haye S, Houghton T, Bauen A, Altmann M, Schmidt P (2021) Options for a UK low carbon hydrogen standard—final report. London
6. UK Government (2021) UK Hydrogen Strategy. London
7. Yin Tee S, Yin Win K, Siang Teo W, Koh L-D, Liu S, Peng Teng C, Han M-Y, Tee SY, Win KY, Koh L, Liu S, Teng CP, Han M, Teo WS (2017) Recent progress in energy-driven water splitting. *Adv Sci*. <https://doi.org/10.1002/advs.201600337>
8. Osman AI, Deka TJ, Baruah DC, Rooney DW (2020) Critical challenges in biohydrogen production processes from the organic feedstocks. *Biomass Convers Biorefinery*. <https://doi.org/10.1007/s13399-020-00965-x>
9. Kawai T, Sakata T (1980) Conversion of carbohydrate into hydrogen fuel by a photocatalytic process. *Nature* 286:474
10. Fujishima A, Honda K (1972) Electrochemical photolysis of water at a semiconductor electrode. *Nature* 238:37–38
11. Inoue TFAKS, Honda K (1979) Photoelectrocatalytic reduction of carbon dioxide in aqueous suspensions of semiconductor powders. *Nature* 277:637–638
12. Jaeger CD, Bard AJ (1979) Spin trapping and electron spin resonance detection of radical intermediates in the photodecomposition of water at titanium dioxide particulate systems. *J Phys Chem* 83:3146–3152. <https://doi.org/10.1021/j100487a017>
13. Bard AJ (1979) Photoelectrochemistry and heterogenous photocatalysis at semiconductors. *J Photochem Photobiol C* 11:59–75

14. Cherubini F (2010) The biorefinery concept: using biomass instead of oil for producing energy and chemicals. *Energy Convers Manage* 51:1412–1421. <https://doi.org/10.1016/J.ENCONMAN.2010.01.015>
15. Royal Society (Great Britain) (2008) Sustainable biofuels: prospects and challenges. 82
16. Colmenares JC (2019) Selective redox photocatalysis: Is there any chance for solar bio-refineries? *Curr Opin Green Sustain Chem* 15:38–46. <https://doi.org/10.1016/J.COAGSC.2018.08.008>
17. Czelej K, Colmenares JC, Jabłczyńska K, Cwieka K, Werner Ł, Gradoń L (2021) Sustainable hydrogen production by plasmonic thermophotocatalysis. *Catal Today* 380:156–186. <https://doi.org/10.1016/J.CATTOD.2021.02.004>
18. Skillen N, McCullagh C, Adams M (2014) Photocatalytic splitting of water. Springer, Berlin, pp 1–42
19. Chen W-T, Chan A, Sun-Waterhouse D, Llorca J, Idriss H, Waterhouse GIN (2018) Performance comparison of Ni/TiO₂ and Au/TiO₂ photocatalysts for H₂ production in different alcohol-water mixtures. *J Catal* 367:27–42
20. Skillen N, Adams M, McCullagh C, Ryu SY, Fina F, Hoffmann MR, Irvine JTS, Robertson PKJ (2016) The application of a novel fluidised photo reactor under UV-Visible and natural solar irradiation in the photocatalytic generation of hydrogen. *Chem Eng J*. <https://doi.org/10.1016/j.cej.2015.10.101>
21. Nakata K, Fujishima A (2012) TiO₂ photocatalysis: design and applications. *J Photochem Photobiol C* 13:169–189
22. Ollis DF, Pelizzetti E, Serpone N (1989) Photocatalysis: fundamentals and applications
23. Fox MA, Dulay MT (1993) Heterogeneous photocatalysis. *Chem Rev* 93:341–357. <https://doi.org/10.1021/cr00017a016>
24. Robertson PKJ (1996) Semiconductor photocatalysis: an environmentally acceptable alternative production technique and effluent treatment process. *J Clean Prod* 4:203–212. [https://doi.org/10.1016/S0959-6526\(96\)00044-3](https://doi.org/10.1016/S0959-6526(96)00044-3)
25. Spasiano D, Marotta R, Malato S, Fernandez-Ibañez P, di Somma I (2015) Solar photocatalysis: materials, reactors, some commercial, and pre-industrialized applications. a comprehensive approach. *Appl Catal B* 170–171:90–123. <https://doi.org/10.1016/j.apcatb.2014.12.050>
26. Mills A, le Hunte S (1997) An overview of semiconductor photocatalysis. *J Photochem Photobiol, A* 108:1–35. [https://doi.org/10.1016/S1010-6030\(97\)00118-4](https://doi.org/10.1016/S1010-6030(97)00118-4)
27. Hoffmann MR, Martin ST, Choi W, Bahnemann DW (1995) Environmental applications of semiconductor photocatalysis. *Chem Rev* 95:69–96. <https://doi.org/10.1021/cr00033a004>
28. Nosaka Y, Nosaka AY (2017) Generation and detection of reactive oxygen species in photocatalysis. *Chem Rev* 117:11302–11336
29. Zhang G, Ni C, Huang X, Welgamage A, Lawton LA, Robertson PKJ, Irvine JTS (2016) Simultaneous cellulose conversion and hydrogen production assisted by cellulose decomposition under UV-light photocatalysis. *Chem Commun* 52:1673–1676. <https://doi.org/10.1039/C5CC09075J>
30. Nwosu U, Wang A, Palma B, Zhao H, Khan MA, Kibria M, Hu J (2021) Selective biomass photoreforming for valuable chemicals and fuels: A critical review. *Renew Sustain Energy Rev*. <https://doi.org/10.1016/j.rser.2021.111266>
31. Liu X, Duan X, Wei W, Wang S, Ni B-J (2019) Photocatalytic conversion of lignocellulosic biomass to valuable products. *Green Chem* 21:4266–4289. <https://doi.org/10.1039/C9GC01728C>
32. Caravaca A, Jones W, Hardacre C, Bowker M (2016) H₂ production by the photocatalytic reforming of cellulose and raw biomass using Ni, Pd, Pt and Au on titania. *Proc R Soc A Math Phys Eng Sci* 472:2
33. Osman AI, Skillen NC, Robertson PKJ, Rooney DW, Morgan K (2020) Exploring the photocatalytic hydrogen production potential of titania doped with alumina derived from foil waste. *Int J Hydrogen Energy*. <https://doi.org/10.1016/j.ijhydene.2020.02.065>
34. Skillen N, Rice C, Pang X, Robertson PKJ, McCormick W, McCrudden D (2021) Photocatalytic radical species: an overview of how they are generated, detected, and measured. *Nanostruct Photocatal*. <https://doi.org/10.1016/B978-0-12-823007-7.00008-0>
35. Chong R, Li J, Ma Y, Zhang B, Han H, Li C (2014) Selective conversion of aqueous glucose to value-added sugar aldose on TiO₂-based photocatalysts. *J Catal* 314:101–108. <https://doi.org/10.1016/j.jcat.2014.03.009>
36. Kim G, Lee S-H, Choi W (2015) Glucose–TiO₂ charge transfer complex-mediated photocatalysis under visible light. *Appl Catal B* 162:463–469

37. Ćwieka K, Czelej K, Colmenares JC, Jabłczyńska K, Werner Ł, Gradoń L (2021) Supported plasmonic nanocatalysts for hydrogen production by wet and dry photoreforming of biomass and biogas derived compounds: recent progress and future perspectives. *ChemCatChem* 13:4458–4496. <https://doi.org/10.1002/cctc.202101006>
38. Wakerley DW, Kuehnel MF, Orchard KL, Ly KH, Rosser TE, Reisner E (2017) Solar-driven reforming of lignocellulose to H₂ with a CdS/CdOx photocatalyst. *Nat Energy* 2:17021
39. Puga A (2016) Photocatalytic production of hydrogen from biomass-derived feedstocks. *Coord Chem Rev* 315:1–66. <https://doi.org/10.1016/J.CCR.2015.12.009>
40. Kondarides DI, Daskalaki VM, Patsoura A, Verykios XE (2008) Hydrogen production by photo-induced reforming of biomass components and derivatives at ambient conditions. *Catal Lett* 122:26–32. <https://doi.org/10.1007/s10562-007-9330-3>
41. Kondarides DI, Patsoura A, Verykios XE (2010) Anaerobic photocatalytic oxidation of carbohydrates in aqueous Pt/TiO₂ suspensions with simultaneous production of hydrogen. *J Adv Oxid Technol*. <https://doi.org/10.1515/jaots-2010-0115>
42. Chang C, Skillen N, Nagarajan S, Ralphs K, Irvine JTS, Lawton L, Robertson PKJ (2019) Using cellulose polymorphs for enhanced hydrogen production from photocatalytic reforming. *Sustain Energy Fuels* 3:1971–1975. <https://doi.org/10.1039/c9se00377k>
43. Lan L, Shao Y, Jiao Y, Zhang R, Hardacre C, Fan X (2020) Systematic study of H₂ production from catalytic photoreforming of cellulose over Pt catalysts supported on TiO₂. *Chin J Chem Eng* 28:2084–2091. <https://doi.org/10.1016/J.CJCHE.2020.03.030>
44. Abdul Razak S, Mahadi AH, Abdullah R, Yasin HM, Jaafar F, Abdul Rahman N, Bahruji H (2020) Biohydrogen production from photodecomposition of various cellulosic biomass wastes using metal-TiO₂ catalysts. *Biomass Convers Biorefin*. <https://doi.org/10.1007/S13399-020-01164-4>
45. Zou J, Zhang G, Xu X (2018) One-pot photoreforming of cellulosic biomass waste to hydrogen by merging photocatalysis with acid hydrolysis. *Appl Catal A* 563:73–79. <https://doi.org/10.1016/J.APCATA.2018.06.030>
46. Speltini A, Sturini M, Dondi D, Annovazzi E, Maraschi F, Caratto V, Profumo A, Buttafava A (2014) Sunlight-promoted photocatalytic hydrogen gas evolution from water-suspended cellulose: a systematic study. *Photochem Photobiol Sci* 13:1410–1419. <https://doi.org/10.1039/C4PP00128A>
47. Cheng Q, Yuan Y-J, Tang R, Liu Q-Y, Bao L, Wang P, Zhong J, Zhao Z, Yu Z-T, Zou Z (2022) Rapid hydroxyl radical generation on (001)-facet-exposed ultrathin anatase TiO₂ nanosheets for enhanced photocatalytic lignocellulose-to-H₂ conversion. *ACS Catal* 12:2118–2125. <https://doi.org/10.1021/acscatal.1c05713>
48. Hao H, Zhang L, Wang W, Zeng S (2018) Facile modification of titania with nickel sulfide and sulfate species for the photoreformation of cellulose into hydrogen. *Chemsuschem* 11:2810–2817. <https://doi.org/10.1002/cssc.201800743>
49. Zhao H, Li CF, Liu LY, Palma B, Hu ZY, Renneckar S, Larter S, Li Y, Kibria MG, Hu J, Su BL (2021) n-p Heterojunction of TiO₂-NiO core-shell structure for efficient hydrogen generation and lignin photoreforming. *J Colloid Interface Sci* 585:694–704. <https://doi.org/10.1016/J.JCIS.2020.10.049>
50. Li C, Naghadeh SB, Guo L, Xu K, Zhang JZ, Wang H (2020) Cellulose as sacrificial biomass for photocatalytic hydrogen evolution over one-dimensional CdS loaded with NiS₂ as a cocatalyst. *ChemistrySelect* 5:1470–1477. <https://doi.org/10.1002/slct.201904840>
51. Li C, Wang H, Naghadeh SB, Zhang JZ, Fang P (2018) Visible light driven hydrogen evolution by photocatalytic reforming of lignin and lactic acid using one-dimensional NiS/CdS nanostructures. *Appl Catal B* 227:229–239. <https://doi.org/10.1016/j.apcatb.2018.01.038>
52. Kasap H, Achilleos D, Huang A, Reisner E (2018) Photoreforming of lignocellulose into H₂ using nanoengineered carbon nitride under benign conditions. *J Am Chem Soc* 140:11604–11607. <https://doi.org/10.1021/jacs.8b07853>
53. Rao C, Xie M, Liu S, Chen R, Su H, Zhou L, Pang Y, Lou H, Qiu X (2021) Visible light-driven reforming of lignocellulose into H₂ by intrinsic monolayer carbon nitride. *ACS Appl Mater Interfaces* 13:44243–44253. <https://doi.org/10.1021/acsami.1c10842>
54. Wang S, Zhang J, Li B, Sun H, Wang S (2021) Engineered graphitic carbon nitride-based photocatalysts for visible-light-driven water splitting: a review. *Energy Fuels* 35:6504–6526. <https://doi.org/10.1021/acs.energyfuels.1c00503>
55. Gao J, Wang Y, Zhou S, Lin W, Kong Y (2017) A facile one-step synthesis of Fe-doped g-C₃N₄ nanosheets and their improved visible-light photocatalytic performance. *ChemCatChem* 9:1708–1715. <https://doi.org/10.1002/cctc.201700492>

56. Anandan S, Pugazhenthiran N, Lana-Villarreal T, Lee GJ, Wu JJ (2013) Catalytic degradation of a plasticizer, di-ethylhexyl phthalate, using Nx-TiO₂-x nanoparticles synthesized via co-precipitation. *Chem Eng J* 231:182–189. <https://doi.org/10.1016/j.cej.2013.07.020>
57. Nguyen V-C, Nimbalkar D, Nam L, Lee Y-L, Teng H, (2021) Photocatalytic cellulose reforming for H₂ and formate production by using graphene oxide-dot catalysts. *ACS Catal* 11:4955–4967. <https://doi.org/10.1021/acscatal.1c00217>
58. Jaswal R, Shende R, Nan W, Shende A (2017) Photocatalytic reforming of pinewood (*Pinus ponderosa*) acid hydrolysate for hydrogen generation. *Int J Hydrogen Energy* 42:2839–2848. <https://doi.org/10.1016/j.ijhydene.2016.12.006>
59. Reilly K, Taghipour F, Wilkinson DP (2012) Photocatalytic hydrogen production in a UV-irradiated fluidized bed reactor. *Energy Proc* 29:513–521. <https://doi.org/10.1016/j.egypro.2012.09.060>
60. Pinaud BA, Benck JD, Seitz LC, Forman AJ, Chen Z, Deutsch TG, James BD, Baum KN, Baum GN, Ardo S, Wang H, Miller E, Jaramillo TF (2013) Technical and economic feasibility of centralized facilities for solar hydrogen production via photocatalysis and photoelectrochemistry. *Energy Environ Sci* 6:1983. <https://doi.org/10.1039/c3ee40831k>
61. Nishiyama H, Yamada T, Nakabayashi M, Maehara Y, Yamaguchi M, Kuromiya Y, Nagatsuma Y, Tokudome H, Akiyama S, Watanabe T, Narushima R, Okunaka S, Shibata N, Takata T, Hisatomi T, Domen K (2021) Photocatalytic solar hydrogen production from water on a 100-m² scale. *Nature* 304:598. <https://doi.org/10.1038/s41586-021-03907-3>
62. Hisatomi T, Domen K (1929) Reaction systems for solar hydrogen production via water splitting with particulate semiconductor photocatalysts. *Nat Catal*. <https://doi.org/10.1038/s41929-019-0242-6>
63. Kawai T, Sakata T (1981) Photocatalytic hydrogen production from water by the decomposition of poly-vinylchloride, protein, algae, dead insects, and excrement. *Chem Lett* 10:81–84. <https://doi.org/10.1246/cl.1981.81>
64. Lan L, Chen H, Lee D, Xu S, Skillen N, Tedstone A, Robertson P, Garforth A, Daly H, Hardacre C, Fan X (2022) Effect of ball-milling pretreatment of cellulose on its photoreforming for H₂ production. *ACS Sustain Chem Eng*. <https://doi.org/10.1021/acssuschemeng.1c07301>
65. Wang L, Zhang Z, Zhang L, Xue S, Doherty WOS, O'Hara IM, Ke X (2015) Sustainable conversion of cellulosic biomass to chemicals under visible-light irradiation. *RSC Adv* 5:85242–85247. <https://doi.org/10.1039/C5RA16616K>
66. Fan H, Li G, Yang F, Yang L, Zhang S (2011) Photodegradation of cellulose under UV light catalysed by TiO₂. *J Chem Technol Biotechnol* 86:1107–1112. <https://doi.org/10.1002/jctb.2632>
67. Sakata T, Kawai T (1981) Photodecomposition of water by using organic compounds. *J Synth Org Chem Jpn* 39:589–602. <https://doi.org/10.5059/yukigoseikyokaiishi.39.589>
68. Kadam SR, Mate VR, Panmand RP, Nikam LK, Kulkarni M, Sonawane RS, Kale BB (2014) A green process for efficient lignin (biomass) degradation and hydrogen production via water splitting using nanostructured C, N, S-doped ZnO under solar light. *RSC Adv* 4:60626–60635. <https://doi.org/10.1039/C4RA10760H>
69. Zhang B, Li J, Guo L, Chen Z, Li C (2018) Photothermally promoted cleavage of β-1,4-glycosidic bonds of cellulosic biomass on Ir/HY catalyst under mild conditions. *Appl Catal B* 237:660–664
70. Colmenares JC (2015) Chapter 8. Nanophotocatalysis in selective transformations of lignocellulose-derived molecules: a green approach for the synthesis of fuels, fine chemicals, and pharmaceuticals. pp 168–201
71. Han G, Yan T, Zhang W, Zhang YC, Lee DY, Cao Z, Sun Y (2019) Highly selective photocatalytic valorization of lignin model compounds using ultrathin metal/CdS. *ACS Catal* 9:11341–11349. <https://doi.org/10.1021/acscatal.9b02842>
72. Nair V, Dhar P, Vinu R (2016) Production of phenolics via photocatalysis of ball milled lignin–TiO₂ mixtures in aqueous suspension. *RSC Adv* 6:18204–18216. <https://doi.org/10.1039/C5RA25954A>
73. Wu X, Fan X, Xie S, Lin J, Cheng J, Zhang Q, Chen L, Wang Y (1929) Solar energy-driven lignin-first approach to full utilization of lignocellulosic biomass under mild conditions. *Nat Catal*. <https://doi.org/10.1038/s41929-018-0148-8>
74. Njiojob CN, Bozell JJ, Long BK, Elder T, Key RE, Hartwig WT (2016) Enantioselective syntheses of lignin models: an efficient synthesis of β-O-4 dimers and trimers by using the evans chiral auxiliary. *Chem Eur J* 22:12506–12517. <https://doi.org/10.1002/chem.201601592>


75. Mukhtar A, Zaheer M, Saeed M, Voelter W (2017) Synthesis of lignin model compound containing a β -O-4 linkage. *Zeitschrift für Naturforschung - Section B Journal of Chemical Sciences* 72:119–124. <https://doi.org/10.1515/znb-2016-0201>
76. Kä Rkã MD, Bosque I, Matsuura BS, Stephenson CRJ (2016) Photocatalytic oxidation of lignin model systems by merging visible-light photoredox and palladium catalysis. <https://doi.org/10.1021/acs.orglett.6b02651>
77. Nguyen J, Matsuura B, Stephenson C (2014) A photochemical strategy for lignin degradation at room temperature. *J Am Chem Soc* 136:1218–1221. <https://doi.org/10.1021/ja4113462>
78. Luo N, Wang M, Li H, Zhang J, Liu H, Wang F (2016) Photocatalytic oxidation-hydrogenolysis of lignin β -O-4 models via a dual light wavelength switching strategy. *ACS Catal* 6:7716–7721. <https://doi.org/10.1021/acscatal.6b02212>
79. Luo J, Zhang X, Lu J, Zhang J (2017) Fine tuning the redox potentials of carbazolic porous organic frameworks for visible-light photoredox catalytic degradation of lignin β -O-4 models. *ACS Catal* 7:5062–5070. <https://doi.org/10.1021/acscatal.7b01010>
80. Murnaghan CWJ, Skillen N, Hardacre C, Bruce J, Sheldrake GN, Robertson PKJ (2021) Exploring lignin valorisation: the application of photocatalysis for the degradation of the β -5 linkage. *J Phys Energy* 3:035002. <https://doi.org/10.1088/2515-7655/abf853>
81. Machado AEH, Furuyama AM, Falone SZ, Ruggiero R, da Silva PD, Castellan A (2000) Photocatalytic degradation of lignin and lignin models, using titanium dioxide: the role of the hydroxyl radical. *Chemosphere* 40:115–124
82. Zakzeski J, Bruijninx PCA, Jongerius AL, Weckhuysen BM (2010) The catalytic valorization of ligning for the production of renewable chemicals. *Chem Rev* 110:3552–3599. <https://doi.org/10.1021/cr900354u>
83. Zhang J (2018) Conversion of lignin models by photoredox catalysis. *Chemsuschem* 11:3071–3080. <https://doi.org/10.1002/cssc.201801370>
84. Kim S, Chmely SC, Nimlos MR, Bomble YJ, Foust TD, Paton RS, Beckham GT (2011) Computational study of bond dissociation enthalpies for a large range of native and modified Lignins. *J Phys Chem Lett* 2:2846–2852. <https://doi.org/10.1021/jz201182w>
85. Luchtefeld R, Dasari MS, Richards KM, Alt ML, Crawford CFP, Schleiden A, Ingram J, Hamidou AAA, Williams A, Chernovitz PA, Sun GY, Luo R, Smith RE (2008) Synthesis of diapocynin. *J Chem Educ* 85:411. <https://doi.org/10.1021/ed085p411>
86. Wang Q, Smith RE, Luchtefeld R, Sun AY, Simonyi A, Luo R, Sun GY (2008) Bioavailability of apocynin through its conversion to glycoconjugate but not to diapocynin. *Phytomedicine* 15:496–503. <https://doi.org/10.1016/j.phymed.2007.09.019>
87. Lei M, Wu S, Liu C, Liang J, Xiao R (2021) Revealing the pyrolysis behavior of 5–5' biphenyl-type lignin fragment. Part I: A mechanistic study on fragmentation via experiments and theoretical calculation. *Fuel Process Technol* 217:106812. <https://doi.org/10.1016/j.fuproc.2021.106812>
88. Kim YS, Chang HM, Kadla JF (2008) Polyoxometalate (POM) oxidation of lignin model compounds. *Holzforschung* 62:38–49. <https://doi.org/10.1515/HF.2008.006>
89. Machado AEH, Furuyama AM, Falone SZ, Ruggiero R, da Perez D, Castellan A (2000) Photocatalytic degradation of lignin and lignin models, using titanium dioxide: the role of the hydroxyl radical. *Chemosphere* 40:115–124. [https://doi.org/10.1016/S0045-6535\(99\)00269-6](https://doi.org/10.1016/S0045-6535(99)00269-6)
90. Murnaghan CWJ, Skillen N, Hardacre C, Bruce J, Sheldrake GN, Robertson PKJ (2021) Exploring lignin valorisation : the application of photocatalysis for the degradation of the β -5 linkage. *J Phys Energy* 3:1–10
91. Banerjee S, Dionysiou DD, Pillai SC (2015) Self-cleaning applications of TiO₂ by photo-induced hydrophilicity and photocatalysis. *Appl Catal B* 176–177:396–428. <https://doi.org/10.1016/J.APCATB.2015.03.058>
92. Liu K, Cao M, Fujishima A, Jiang L (2014) Bio-inspired titanium dioxide materials with special wettability and their applications. *Chem Rev*. <https://doi.org/10.1021/cr4006796>
93. Villa K, Domènech X, Malato S, Maldonado MI, Peral J (2013) Heterogeneous photocatalytic hydrogen generation in a solar pilot plant. *Int J Hydrog Energy* 38:12718–12724. <https://doi.org/10.1016/j.ijhydene.2013.07.046>
94. Arzate Salgado SY, Ramírez Zamora RM, Zanella R, Peral J, Malato S, Maldonado MI (2016) Photocatalytic hydrogen production in a solar pilot plant using a Au/TiO₂ photo catalyst. *Int J Hydrogen Energy* 41:11933–11940. <https://doi.org/10.1016/j.ijhydene.2016.05.039>

95. Rumayor M, Corredor J, Rivero MJ, Ortiz I (2022) Prospective life cycle assessment of hydrogen production by waste photoreforming. *J Clean Prod* 336:130430. <https://doi.org/10.1016/J.CLEPRO.2022.130430>
96. Cassano AE, Alfano OM (2000) Reaction engineering of suspended solid heterogeneous photocatalytic reactors. *Catal Today* 58:167–197. [https://doi.org/10.1016/S0920-5861\(00\)00251-0](https://doi.org/10.1016/S0920-5861(00)00251-0)
97. van Gerven T, Mul G, Moulijn J, Stankiewicz A (2007) A review of intensification of photocatalytic processes. *Chem Eng Process* 46:781–789. <https://doi.org/10.1016/j.ccep.2007.05.012>
98. Braham R, Harris A (2009) Review of major design and scale-up considerations for solar photocatalytic reactors. *Ind Eng Chem Res* 48:8890–8905. <https://doi.org/10.1021/ie900859z>
99. McCullagh C, Skillen N, Adams M, Robertson PK (2011) Photocatalytic reactors for environmental remediation: a review. *J Chem Technol Biotechnol*. <https://doi.org/10.1002/jctb.2650>
100. Sundar KP, Kanmani S (2020) Progression of photocatalytic reactors and its comparison: a review. *Chem Eng Res Des* 154:135–150. <https://doi.org/10.1016/j.cherd.2019.11.035>
101. Turchi C, Ollis D (2002) Comment. Photocatalytic reactor design: an example of mass-transfer limitations with an immobilized catalyst. *J Phys Chem* 92:6852–6853. <https://doi.org/10.1021/j100334a070>
102. Dijkstra MFJ, Michorius A, Buwalda H, Panneman HJ, Winkelman JGM, Beenackers AACM (2001) Comparison of the efficiency of immobilized and suspended systems in photocatalytic degradation. *Catal Today* 66:487–494. [https://doi.org/10.1016/S0920-5861\(01\)00257-7](https://doi.org/10.1016/S0920-5861(01)00257-7)
103. Ballari de los M, Alfano OM, Cassano AE (2010) Mass transfer limitations in slurry photocatalytic reactors: experimental validation. *Chem Eng Sci* 65:4931–4942. <https://doi.org/10.1016/j.ces.2010.04.021>
104. Timmerhuis NAB, Wood JA, Lammertink RGH (2021) Connecting experimental degradation kinetics to theoretical models for photocatalytic reactors: the influence of mass transport limitations. *Chem Eng Sci* 245:116835. <https://doi.org/10.1016/j.ces.2021.116835>
105. Mo J, Zhang Y, Yang R, Xu Q (2008) Influence of fins on formaldehyde removal in annular photocatalytic reactors. *Build Environ* 43:238–245. <https://doi.org/10.1016/j.buildenv.2005.12.027>
106. Adams M, Campbell I, Robertson PKJ (2008) Novel photocatalytic reactor development for removal of hydrocarbons from water. *Int J Photoenergy* 2008:1–7. <https://doi.org/10.1155/2008/674537>
107. Amiri H, Ayati B, Ganjidoust H (2017) Mass transfer phenomenon in photocatalytic cascade disc reactor: Effects of artificial roughness and flow rate. *Chem Eng Process* 116:48–59. <https://doi.org/10.1016/j.ccep.2017.03.004>
108. Abidi M, Hajjaji A, Bouzaza A, Lamaa L, Peruchon L, Brochier C, Rtimi S, Wolbert D, Bessais B, Assadi AA (2022) Modeling of indoor air treatment using an innovative photocatalytic luminous textile: Reactor compactness and mass transfer enhancement. *Chem Eng J* 430:132636. <https://doi.org/10.1016/j.cej.2021.132636>
109. Meng X, Yun N, Zhang Z (2019) Recent advances in computational photocatalysis: A review. *Can J Chem Eng* 97:1982–1998. <https://doi.org/10.1002/cjce.23477>
110. Loeb SK, Alvarez P, Brame J, Cates E, Choi W, Crittenden J, Dionysiou D, Li Q, Li-Puma G, Quan X, Sedlak D, David Waite T, Westerhoff P, Kim J-H (2018) The technology horizon for photocatalytic water treatment: sunrise or sunset? *Environ Sci Technol* 53:2937–2947. <https://doi.org/10.1021/acs.est.8b05041>
111. Fife Council (2022) H100 Fife. <https://www.sgn.co.uk/H100Fife>. Accessed 26 May 2022
112. Bowker M (2019) Methanol synthesis from CO₂ hydrogenation. *ChemCatChem* 11:4238–4246. <https://doi.org/10.1002/cctc.201900401>
113. Uekert T, Dorchies F, Pichler CM, Reisner E (2020) Photoreforming of food waste into value-added products over visible-light-absorbing catalysts. <https://doi.org/10.1039/d0gc01240h>
114. Uekert T, Kasap H, Reisner E (2019) Photoreforming of nonrecyclable plastic waste over a carbon nitride/nickel phosphide catalyst. *J Am Chem Soc* 141:15201–15210. <https://doi.org/10.1021/jacs.9b06872>
115. Xu S, Chen H, Hardacre C, Fan X (2021) Non-thermal plasma catalysis for CO₂ conversion and catalyst design for the process. *J Phys D Appl Phys* 54:233001. <https://doi.org/10.1088/1361-6463/abe9e1>
116. Chen H, Mu Y, Xu S, Xu S, Hardacre C, Fan X (2020) Recent advances in non-thermal plasma (NTP) catalysis towards C1 chemistry. *Chin J Chem Eng* 28:2010–2021. <https://doi.org/10.1016/J.CJCHE.2020.05.027>
117. Xu S, Chansai S, Shao Y, Xu S, Wang YC, Haigh S, Mu Y, Jiao Y, Stere CE, Chen H, Fan X, Hardacre C (2020) Mechanistic study of non-thermal plasma assisted CO₂ hydrogenation over Ru supported on MgAl layered double hydroxide. *Appl Catal B Environ* 268:118752. <https://doi.org/10.1016/J.APCATB.2020.118752>

118. Sathre R, Scown CD, Morrow WR, Stevens JC, Sharp ID, Ager JW, Walczak K, Houle FA, Greenblatt JB (2014) Life-cycle net energy assessment of large-scale hydrogen production via photoelectrochemical water splitting. *Energy Environ Sci* 7:3264–3278. <https://doi.org/10.1039/C4EE01019A>
119. Leblebici ME, Stefanidis GD, van Gerven T (2015) Comparison of photocatalytic space-time yields of 12 reactor designs for wastewater treatment. *Chem Eng Process* 97:106–111

Publisher's Note Springer Nature remains neutral with regard to jurisdictional claims in published maps and institutional affiliations.

Authors and Affiliations

Nathan Skillen¹ · **Helen Daly**² · **Lan Lan**² · **Meshal Aljohani**² · **Christopher W. J. Murnaghan**¹ · **Xiaolei Fan**² · **Christopher Hardacre**² · **Gary N. Sheldrake**¹ · **Peter K. J. Robertson**¹ 

✉ Nathan Skillen
n.skillen@qub.ac.uk

✉ Peter K. J. Robertson
p.robertson@qub.ac.uk

¹ School of Chemistry and Chemical Engineering, Queens University Belfast, David Keir Building, Stranmillis Road, Belfast BT9 5AL, UK

² Department of Chemical Engineering, School of Engineering, The University of Manchester, Oxford Road, Manchester M13 9P3AL, UK